ISTANBUL TECHNICAL UNIVERSITY ★ GRADUATE SCHOOL OF SCIENCE ENGINEERING AND TECHNOLOGY

NUMERICAL INVESTIGATION AND THERMAL ANALYSIS OF SOLAR CAVITY RECEIVER

M.Sc. THESIS

Selin BİLMEZ

Department of Aeronautics and Astronautics Engineering

Aeronautics and Astronautics Engineering Programme

JUNE 2018

ISTANBUL TECHNICAL UNIVERSITY ★ GRADUATE SCHOOL OF SCIENCE ENGINEERING AND TECHNOLOGY

NUMERICAL INVESTIGATION AND THERMAL ANALYSIS OF SOLAR CAVITY RECEIVER

M.Sc. THESIS

Selin BİLMEZ
(511161147)

Department of Aeronautics and Astronautics Engineering

Aeronautics and Astronautics Engineering Programme

Thesis Advisor: Prof. Dr. A. Cihat BAYTAŞ

JUNE 2018

ISTANBUL TEKNİK ÜNİVERSİTESİ ★ FEN BİLİMLERİ ENSTİTÜSÜ

GÜNEŞ IŞINI ALICI KABININ SAYISAL İNCELENMESİ VE ISIL ANALİZİ

YÜKSEK LİSANS TEZİ

Selin BİLMEZ
(511161147)

Uçak ve Uzay Mühendisliği Anabilim Dalı

Uçak ve Uzay Mühendisliği Programı

Tez Danışmanı: Prof. Dr. A. Cihat BAYTAŞ

HAZİRAN 2018

Selin BİLMEZ, a M.Sc. student of ITU Graduate School of Science Engineering and Technology student ID 511161147, successfully defended the thesis/dissertation entitled "NUMERICAL INVESTIGATION AND THERMAL ANALYSIS OF SOLAR CAVITY RECEIVER", which he/she prepared after fulfilling the requirements specified in the associated legislations, before the jury whose signatures are below.

Thesis Advisor :	**Prof. Dr. A. Cihat BAYTAŞ** Istanbul Technical University	.....
Jury Members :	**Assist. Prof. Dr. Bayram ÇELİK** Istanbul Technical University	.....
	Assist. Prof. Dr. Şule KAPKIN Istanbul University	.....

Date of Submission : 04 May 2018
Date of Defense : 08 June 2018

To my family,

FOREWORD

I would like to thank to my family for supporting me for two years of this master education and thesis study. I also would like to thank to my advisor Prof. Dr. A. Cihat Baytaş for sharing me his valuable knowledge and experience about the thesis subject.

May 2018

Selin BİLMEZ
(Aerospace Engineer and Chemist)

TABLE OF CONTENTS

Page

ABBREVIATIONS

in	**:** into cavity
∞	**:** ambient value
H	**:** hot wall
$\mathbf{T_w}$	**:** is the temperature of the hot wall
Ra	**:** Rayleigh number
cond	**:** conduction heat transfer
conv	**:** convection heat transfer
r	**:** radiation heat transfer
$\mathbf{Nu_x}$	**:** local Nusselt number
$\mathbf{Nu_c}$	**:** convective Nusselt number
$\mathbf{Nu_r}$	**:** radiative Nusselt number
max	**:** maximum
min	**:** minimum

SYMBOLS

A : enclosure aspect ratio, H/L

AP : dimensionless aperture position, d/H

AR : dimensionless aperture size, h/H

Cp : heat capacity, J/kg K

g : acceleration due to gravity, m/s^2

H : cavity height, m

k : thermal conductivity of fluid, W/m K

h : convection heat transfer coefficient (W/m^2K)

L : cavity width, m

Nu : Nusselt number

p : pressure, Pa

Pr : Prandtl number, υ/α

Ra : Rayleigh number, $gb\Delta TL^3/(\upsilon\alpha)$

t : time, s

ΔT : temperature difference, $(T - T_\infty)$

u,v : fluid velocities

x,y : Cartesian coordinates

W : Watt

α : thermal diffusivity, m^2/s

β : thermal expansion coefficient, 1/K

υ : kinematic viscosity, m^2/s

μ : dynamic viscosity, Ns/m^2

ρ : fluid density, kg/m^3

φ : inclination angle of the heated wall from the horizontal, ^{o}

σ : Boltzman constant, 5,67 x 10-8 $W/m^2 K^4$

δ : thickness of the velocity boundary layer

δt : thickness of the thermal boundary layer

ε : emissivity of the material

LIST OF TABLES

Page

LIST OF FIGURES

Page

NUMERICAL INVESTIGATION AND THERMAL ANALYSIS OF SOLAR CAVITY RECEIVER

SUMMARY

The purpose of this thesis is to investigate steady, laminar, combined pure natural convection and surface radiation in a tilted 2D solar square cavity receiver, perform thermal analysis by using ANSYS Fluent, and compare the results with published ones and to be able to offer a new solution to the investigated reasons of thermal losses. This study is important to propose an optimum thermal design for solar concentrators. 2D solar square cavity receiver has a constantly heated left wall, and insulated top and bottom wall and an opening right wall. The temperature of the heated left wall is 350 K and temperature of the air coming from opening wall is 300 K, so the temperature difference investigated for the solar cavity receiver is 50 K. Different Rayleigh numbers from 10^2 to 10^6 were studied. Parameter changed for Rayleigh number depends on the factor investigated in the different cases for this study, such as it could be gravity or dimension.

2D, laminar, steady state flow, with SIMPLE scheme, presssure-based solver was studied and for air density, Boussinesq approach was applied. Operating temperature, density and pressure were defined as ambient airflow and for Radiation mode, S2S method was used. The default values for the relaxation factors were applied. The residual for continuity, x-momentum, y- momentum convergence criteria was taken as 10^{-3}, on the other hand, for energy convergence it was taken as 10^{-6}.

In this thesis, in order to study the solar cavity receiver, six types of validation studies were performed for validating the mathematical model and boundary conditions used at both numerical calculations and ANSYS Fluent. The numerical and thermal analysis for both pure natural convection and combined natural convection and surface radiation were studied for finding the main reasons of thermal losses. In all the validation studies, the computed Nusselt numbers were validated with the published ones.

The first validation study was for a pure natural convection analysis in a closed square cavity. The results indicated that, as Rayleigh number increases, the fluid velocity increases and fluid gets more close to the walls of the cavity and thermal boundary layer and velocity boundary layer thicknesses decrease. The heated fluid circulates in clockwise direction in the cavity because of the buoyancy effect.

The second validation study was to investigate the pure natural convection heat transfer in a fully open square cavity. A fully open, 2D, square cavity thermal analysis was performed by just changing the opening wall boundary condition as pressure inlet. The velocity vector results indicated that fluid enters from bottom part of the cavity, reaches to the hot wall, gets heated, and exits from right side of the top wall of the cavity by buoyancy effect. There forms both thermal boundary layer and

velocity boundary layer near the hot wall but as the Rayleigh number increases the thicknesses of these boundary layers' decrease.

The third validation study was to investigate the tilt angle of open cavity effect on the pure natural convection heat transfer. The result showed that, the minimum natural convection heat loss occurs when $\varphi = 180^{o}$, whereas, the maximum heat loss occurs when $\varphi = 60^{o}$ for the Rayleigh numbers of 10^{3} and 10^{4}, and when $\varphi = 75^{o}$ for the Rayleigh numbers of 10^{5} and 10^{6}. As the tilt angle increases up to $\varphi = 60^{o}$ for $Ra = 10^{3}$ and 10^{4} and up to $\varphi = 75^{o}$ for $Ra = 10^{5}$ and 10^{6}, the heat loss increases slightly and then after that angles the heat loss decreases as dramatically.

The fourth validation was to investigate the effect of opening ratio of cavity aperture on the natural convection heat transfer. The Nusselt numbers calculated for a partially open square cavity were compared with the ones for a fully open square cavity and then the optimum one was discussed for the heat loss reduction. In addition, isotherms and streamlines of a partially open square cavity were validated by comparing with the published results of study of Bilgen and Oztop. The result indicated that increasing the aperture size of the cavity increases the heat loss, so that using a partially open square cavity can reduce the heat loss.

Finally, the last two validation studies were to validate the radiative model (S2S) used and to validate the Nusselt numbers found from combined heat transfer analysis by comparing with the published ones. The validation succeeded and the results indicated that, as the Rayleigh number increases, heat loss increases and radiation heat loss becomes dominant at high Rayleigh numbers.

After validation studies, thermal losses in a solar cavity receiver were investigated by analyzing different parameters such as temperature difference, cavity dimension and cavity tilt angle. The temperature difference and dimension changing of cavity were studied just for $Ra=10^{6}$ and the results were discussed for investigating the heat loss. The results indicated that, as temperature difference increases, the heat loss increases mostly due to radiation heat loss. The Nusselt number for radiation increases dramatically as increasing the temperature of the hot wall, on the other hand, the Nusselt number for natural convection remains almost same. The increase in the length of the solar square cavity makes radiation heat loss dominant because the heat loss of convection decreases from % 97 to % 42. The results of the study performed for investigation of the tilt angle effect on the heat loss in solar cavity indicated that there is a nonlinear relationship with heat loss and tilt angle.

To come up, background of a cavity such as a closed cavity and then an open cavity were studied. Different cases of open cavity were studied such as a fully open cavity, a partially open cavity, an inclined open cavity and all the results were compared with the published similar studies, and the best optimum cavity model at the highest thermal performance was proposed. Both pure natural and combined heat losses were studied and the dominant one was determined.

GÜNEŞ IŞINI ALICI KABININ SAYISAL İNCELENMESİ VE ISIL ANALİZİ

ÖZET

Bu tez çalışmasında amaç, güneş enerjisini toplayarak ısı enerjisine çeviren ve ısıtma sistemlerinde kullanılmasını sağlayan, güneş kollektörlerinin önemli bir parçası olan güneş ışını alıcı kabını incelemek ve yenilebilir bir enerji kaynağı olan güneşten sağlanabilecek enerjinin maksimum seviyede kullananılması için çözümler sunmaktır. Güneş enerjisinden sağlanan verimi artırmak için, güneş ışını alıcı kabında doğal taşınım, ışıma ve rüzgâr gibi dış etkenler yüzünden meydana gelen ısı kayıplarının azaltılması gerekmektedir. Bu amaçla öncelikle güneş ışını alıcı kabı için literatürde yapılan çalışmalar incelenmiş ve ısı kaybına sebep olan ana etkenler belirlenmiştir. Öncelikle güneş ışını alıcı kabının şekli belirlenmiştir. Bunun için literatürdeki çalışmalar incelenmiş ve en az ısı kaybı olan kap şeklinin kare olduğu anlaşılmıştır. 2 boyutlu, eğimli, kare şeklindeki güneş ışını alıcı kabı için literatürde yapılmış ısı transferi analiz çalışmaları incelenmiş ve bu tez çalışmasında ANSYS Fluent kullanılarak analizler yapılmış ve literatürdeki benzer çalışma sonuçları ile karşılaştırılarak sonuçlar doğrulanmıştır.

Bu tez çalışmasının motivasyon noktası, 2 boyutlu, kare bir kapta izolasyon ve sıcak duvar malzemelerininin gerçek ışıma yayma değerleri tanımlanmış ve bu değerler kullanılarak ısı kaybına neden olan farklı etkenler analiz edilmiştir. Güneş kollektörü üreticileri için en uygun güneş ışını alıcı kabı tasarımı ve üretimi için faydalı önerilerde bulunulmuştur.

Bu tez çalışmasında güneş ışını alıcı kabı, 2 boyutlu, kare şeklinde, sol duvardan sabit ısı akısı ile ısıtılıp, üst ve alt duvarları yalıtılmış, sağ duvarı ise açık olarak modellenmiştir. Isıtılan sol duvarın sıcaklığı 350 K, açık olan duvardan gelen havanın sıcaklığı ise 300 K dir, güneş ışını alıcı kabının sıcaklık farkı da 50 K dir. 10^2 den 10^6 kadar farklı Rayleigh sayıları için çalışma yapılmıştır. Rayleigh sayısı için değiştirilen parametre ya yerçekimi ya da kap boyutu olmuştur. Akışkan için yapılan varsayımlar, sıkıştırılamaz, sabit halde ve laminer akış olduğudur. Akışkanın özkütlesi için Boussinesq yaklaşımı kullanılmıştır. Kap duvarlarında kayma ihmal edilmiştir.

Güneş ışını alıcı kabını çalışmak için, hesaplamalarda ve ANSYS Fluent'te kullanılan matematik model ve sınır koşullarını doğrulamak için 6 tip doğrulama çalışması yapılmıştır. Isı kayıplarının temel nedenlerini bulmak için hem saf doğal taşınım hem de doğal taşınım ve yüzey ışımasının birleşiminden meydana gelen birşelik ısı transferi için hesaplamalar ve analizler yapılmıştır. Analizlerde kapalı kap, tam açık kap, eğimli tam açık kap ve kısmi olarak açık kap olmak üzere 4 tip geometri kullanılmıştır. 4 tip geometri için sınır koşulları ve başlangıç koşulları belirlenerek ısı transferi analizleri yapılmıştır. Farklı tip geometrilerde yapılan bu analizlerin bir kısım sonuçları birbiri ile karşılaştırılmış ve ısı kaybını önlemek için doğru geometri

belirlenmeye çalışılmıştır. Tüm doğrulama çalışmalarında Nusselt sayıları, literatürde yayınlanmış benzer çalışma sonuçları ile karşılaştırılıp doğrulanmıştır.

İlk doğrulama çalışması kapalı kare bir kapta saf doğal taşınım analizidir. Düşük Rayleigh sayılarında iletim baskın iken, yüksek Rayleigh sayılarında taşınımın baskın hale geldiği gözlemlenmiştir. Bu durumu, Rayleigh sayısı arttıkça, akışkanın hızının artması ve kap duvarlarına daha fazla yaklaşarak ve hız sınır tabaka kalınlığının azalması kanıtlamaktadır. Ayrıca Rayleigh sayısı arttıkça, sıcak duvar üzerindeki sıcaklık gradyanının arttığı, sıcak duvar üzerinde ısıl sınır tabaka kalınlığının azaldığı gözlemlenmiştir. Isınan akışkan kap içerisinde kaldırma kuvveti etkisi sebebiyle saat yönünde dolaşmaktadır.

İkinci doğrulama çalışması tamamıyla açık olan kare bir kapta doğal taşınımla ısı transferi incelenmesidir. Tamamıyla açık olan 2 boyutlu bir kabın tamamıyla kapalı bir kaptan farklı olarak, sadece açık duvarının sınır koşulu basınç girişi olarak değiştirilip analiz edilmiştir. Basınç dağılımı sonuçları, kabın üst duvarına yakın kısmında soldan sağa doğru, aynı şekilde sağ üst köşeden sol alt köşeye doğru ve sağ alt duvardan sol alt duvara doğru da bir basınç azalması olduğunu göstermektedir. Akışkanlar, basıncın yüksek olduğu yerden düşük olduğu yere doğru hareket eder bu sebeple de, üst duvarın solundan sağına doğru ve sağ üst köşeden, sağ alt köşeye doğru ve sağ alt duvardan sol alt duvara doğru bir akışkan akışı meydana gelmektedir. Akışkan hareket yönü saat yönündedir. Hız vektör sonuçları, akışkanın kabın alt kısmından girdiğini, sıcak duvara ulaştığında ısındığını ve kaldırma kuvveti etkisi ile kabın üst sağ kısmından çıktığını gösteriyor. Açık kapta, sıcak duvar yakınında hem ısıl hem de hız sınır tabakaları oluşur ve Rayleigh sayısı arttıkça bu tabakaların kalınlıkları azalır.

Üçüncü doğrulama çalışmasında açık kap eğim açısının doğal taşınım üzerindeki etkisi incelemiştir. Sonuçlar gösteriyor ki, bütün Rayleigh sayıları için en az ısı kaybı eğim açısı $\varphi = 180^{o}$ olduğunda, en çok ısı kaybı ise, Rayleigh sayısı 10^3 ve 10^4 için eğim açısı $\varphi = 60^{o}$, ve Rayleigh sayısı 10^5 ve 10^6 için eğim açısı $\varphi = 75^{o}$ olduğunda meydana gelir. Rayleigh sayısı 10^3 ve 10^4 için, eğim açısı $\varphi = 60^{o}$ 'ye kadar arttıkça ve Rayleigh sayısı 10^5 ve 10^6 için eğim açısı $\varphi = 75^{o}$ 'e kadar arttıkça, ısı kaybı azar azar artarken, bu açılardan sonra ısı kaybı dramatik bir şekilde düşmeye başlar.

Dördüncü doğrulama çalışması kabın hava giriş açıklık oranının doğal taşınım ısı transferi üzerine olan etkisini incelemektir. Kısmi olarak açık olan kare kap için hesaplanan Nusselt sayıları, tamamen açık olan kare kap için olanlar ile karşılaştırılmış ve ısı kaybı azaltımı için en uygun olan tartışılmıştır. Ayrıca, kısmi olarak açık olan kabın sıcaklık ve hız dağılımları Bilgen ve Öztop' un çalışmasının yayınlanmış sonuçları ile karşılaştırılıp doğrulanmıştır. Sonuçlar, kap giriş açıklığının artması ile ısı kaybının artacağını göstermiştir ve bundan dolayı, kısmi olarak açık kare bir kap kullanmak ısı kaybını azaltır.

Son olarak, son iki doğrulama çalışması ışınım modeli doğrulama ve birleşik ısı transfer analizinden bulunan Nusselt sayılarının yayınlanmış sonuçlarla karşılaştırılmasıdır. Doğrulama başarılıdır ve sonuçlar, Rayleigh sayısının artışı ile ısı kaybının artacağı ve ışıma ile ısı kaybının yüksek Rayleigh sayılarında baskın olduğunu göstermiştir.

Doğrulama çalışmalarından sonra, güneş ışını alıcı kabının ısı kayıplarını incelemek için sıcaklık farkı, kap boyutu ve kap eğim açısı gibi farklı parametrelerin analizleri yapılmıştır. Sıcaklık farkı ve kap boyutu değişikliği sadece $Ra = 10^6$ için çalışılmıştır. Sonuçlar gösteriyor ki, sıcaklık farkı arttıkça, ısı kaybı daha çok ışıma ısı kaybı

sebebiyle artar. Işıma Nusselt sayısı, sıcak duvarın sıcaklığının artması ile dramatik bir şekilde artar iken, doğal taşınım Nusselt sayısı tamamen aynı kalmaktadır. Kare şeklindeki güneş ışını alıcı kabının boyutundaki artış, konveksiyonla ısı kaybını %97' den %42' lere düşürerek, ışımayla ısı kaybının baskın olmasına neden olur. Kap eğim açısının ısı kaybına olan etkisini incelemek için yapılan çalışma, ısı kaybı ile eğim açısı arasında doğrusal olmayan bir ilişki olduğunu göstermiştir. Ayrıca, kap duvarlarında kullanılan malzemelerin ışıma yayma değerlerindeki artış ile ışıma ile ısı kaybı artarak, kap içindeki toplam ısı kaybını arttırmaktadır.

Bu çalışmalardan elde edilen sonuca göre, güneş ışını alıcı kabı içinde meydana gelen ısı kayıplarını azaltmak için, kısmi olarak açık bir kap kullanılabilir. Bu kısmi açık kabın küçük boyutlarda ve düşük ışıma yayma değerlerine sahip malzemelerden yapılması gerekmektedir. Buna ek olarak, bulunulan ortam için hesaplanan Rayleigh sayısına göre en düşük ısı kaybına yol açan uygun eğim açısısı kullanılmalıdır.

Sonuç olarak, kapalı kare bir kap gibi bir kabın ısı transferi analizlerinden sonra ve açık bir kap için çalışma başlatılmıştır. Açık kap için tamamıyla açık kap, kısmi açık kap ve eğimli açık kap gibi farklı durumlar çalışılmıştır ve sonuçların doğrulanması için yayınlanmış sonuçlarla karşılaştırılmışlardır ve en yüksek termal performansa sahip güneş ışını alıcı kap modeli önerilmiştir. Hem saf doğal taşınım ısı kaybı hem de birleşik ısı kayıpları çalışılmış ve baskın olan belirlenmiştir.

1. INTRODUCTION

1.1 Solar Collectors

A solar collector is an energy exchanger used to convert solar irradiation energy to thermal energy or electric energy in PV applications. In this study, solar collectors used for thermal energy were investigated. The thermal solar energy collector function is absorbing heat of solar irradiation by a solar collector and then transferring it to the working fluid. The working fluid can be air, water or oil. There are two types of solar collectors according to concentration ratios. They are non-concentrating collectors and concentrating collectors. In order to increase the thermal performance of the collector heat loss from the absorber should be reduced. The useful energy output of the collector is equal to the difference between the absorbed solar radiation and the total thermal losses from the collector.

1.2 Solar Cavity Receivers

Thermal receiver function is to convert solar heat to the water or engine depending on the application used, and there occurs a heat loss from receiver, which reduces the efficiency of the system so it is very important to have a high thermal performance of a receiver. The heat losses in solar cavity receiver occur because of the convection and radiation heat losses to the air in the cavity and conduction heat losses in the insulation. The cavity wall temperature, the shape factors and emissivity/ absorptivity of the receiver walls affect the radiation heat loss and on the other hand, temperature of the receiver and insulation material affects conduction. On the other hand, there are too many factors affect the convection heat loss of the cavity receivers as the air temperature within the cavity, the inclination of the cavity, the external wind conditions and the cavity geometries. In the literature, the mostly studied shapes of receivers are cubical, rectangular, cylindrical and hemispherical shapes. In this study, a 2D square cavity receiver was studied for different inclination angles.

1.3 Solar Receivers Applications

The solar receiver function is to absorb the concentrated solar energy and then transfers the heat to a working fluid. The receiver thermal efficiency has a significant influence on the overall efficiency of the facility. In this thesis a square solar receiver cavity was investigated for low temperature difference of $\Delta T = 50$ K. The solar energy used applications are listed below [20]:

Heating applications (50–70 ^{o}C)

- Domestic hot water production (~50 ^{o}C)
- Space heating applications (50–70 ^{o}C)
- Drying applications (50–70 ^{o}C)

Water treatment applications

- Stills (40–80 ^{o}C)
- Desalination (70–100 ^{o}C)

Cooling/refrigeration with sorption machines (80–150 ^{o}C)

- Single-stage machines (80 ^{o}C)
- Multistage machines (150 ^{o}C)

Power production applications (100–600 ^{o}C)

- Low-/medium-grade power production, for instance in organic Rankine cycles (100 - 300 ^{o}C)
- High-grade power production, for instance in water/ steam Rankine cycles (300–600 ^{o}C)
- Hybrid power cycles with gas turbines (~600 ^{o}C)

Industrial heat, for instance, steam production (50–400 ^{o}C)

- Washing procedures (90 ^{o}C)
- Chemicals production (200 ^{o}C)
- Methanol reforming (~300 ^{o}C)

Therefore, in this thesis, the receivers mostly can be used at heating applications and water treatment system were analysed.

1.4 Motivation of Work

The receiver is an important tool to transfer concentrated solar heat to the water, so that the heat loss from the receiver plays a significant role in reducing the solar

collector efficiency. It is therefore important to investigate the difference parameters effects on the receiver. There is a lot of research about the reasons of heat loss in the cavities. However, there is a still open research area for heat losses of cavity receivers. The present study therefore focused on the investigation and thermal analysis of solar cavity receiver for different parameters such as Rayleigh numbers, dimensions of cavity, inclination angle, opening ratio and temperature differences effects. The primary approach of this study is to validate the mathematical model by comparing the results with published ones. The first validation study was to validate a closed square cavity and to validate mathematical model of a solar cavity receiver. Then, the second step is to repeat the thermal analysis for different parameters on a square solar cavity receiver. The focus of this thesis after several validation studies is to investigate the temperature difference, cavity dimension changing and inclination angle effects on the heat loss in solar cavity receiver with the defined emissivity values of copper material used for hot wall and wood material used for insulated wall. Actually, with these defined exact values of emissivity for hot and insulated wall materials, there is not any research to compare, so that with these results manufactures whose use wood and copper in a solar cavity receiver may be careful to design and manufacture the optimum cavity receiver.

1.5 Purpose of Thesis

The purpose of this thesis is to investigate a 2D, square solar cavity receiver and perform thermal analysis for a laminar, incompressible and steady state flow, taking into account both pure natural convection and combined natural convection and surface radiation. Different cases for a square solar cavity were studied such as inclined solar cavity, different dimensions of solar cavity, partially open square solar cavity and temperature difference effect. The results of this thesis study will provide a comprehensive understanding of how different parameters affect the performance of the square solar cavity receivers. To sum up, those results will help manufacturers to design and manufacture a solar cavity receiver with efficient performance.

1.6 Literature Survey

In this section, a detailed literature review on past research investigation about heat losses in open and closed square cavities were performed. The literature survey was

separated in terms of the parameters investigated in an open cavity and closed cavity. The most of the literature survey investigations have the similar properties of assumptions for the fluid flow that it is 2D, laminar, steady state and incompressible and Boussinesq approach was applied.

Therefore, the literature surveys are about pure natural convection analysis in open and closed square cavities and combined pure natural convection and surface radiation analysis in open square cavities. Since, the solar cavity receiver shape was chosen as square, both pure natural convection heat transfer and combined heat transfer were studied, and all parameters analysis results were compared with literature.

Pure natural convection investigations

- **A closed square cavity**

Elatar et al. [1] investigated the laminar natural convection inside a square enclosure with a single horizontal fin attached to its hot wall. The left wall of square cavity is hot, horizontal walls are adiabatic and the right wall is cold. Prandtl number for the enclosure is 0.71. The changing parameters were Rayleigh number, fin length, conductivity ratio, thickness and position. The fluid was assumed Newtonian and incompressible and Boussinesq approach was applied for density of the fluid. The central difference discretization was used and it was solved by Gauss-Seidel method. The iteration method used was a line by line consists of from both direct method and Tri Diagonal Matrix Algorithm. They found that the fin thickness has negligible effect on the average Nusselt number for all values of fin conductivity ratios. Increasing the fin length enhances the fin efficiency. The maximum fin efficiency was found at low Rayleigh number. Bairi [2] studied the natural convection in air filled 2D square cavities both experimentally and numerically. The hot and cold wall of the cavity has a constant temperature and the other walls are adiabatic. The conservation of equations was solved by finite volume method. The changing parameters of the problem was Rayleigh number (Ra) and angles of inclination (α). They compared calculated Nu (average) with measured Nu_m (average numbers) for different Ra and α.

- **A fully open rectangular cavity**

Karakaya and Durmuş [3] studied the natural convection heat transfer in rectangular open cavity. They studied both experimentally and numerically. Fluent was used to model the problem and solve the conservation of equations and for simulations. The changing parameter of the problem was Rayleigh number from 10^3 to 10^6. They compared their Nusselt number results calculated from Fluent data's, with the published ones. Kumar [4] studied both the numerical and experimental investigation of the natural convection in 2D open channels. The flow was assumed 2D, laminar and a Boussinesq approximation was applied due to low temperature differences. Fluent was used to solve the conservation of equations with variable properties and slip conditions. The Nusselt number, velocity and temperature profiles and heat transfer rate were compared with the published results for validation of the mathematical model.

- **A partially open inclined 2D square cavity**

Bilgen and Oztop [5] studied the natural convection heat transfer in a partially inclined 2D square cavity. The wall facing the opening is hot and top and bottom walls are adiabatic. They studied a 2D, laminar, steady state, heat transfer by natural convection. They neglected the radiation effects. Their changing parameters for this study was Rayleigh numbers from 10^3 to 10^6 and dimensionless aperture sizes from 0.25 to 0.75, aperture position at high, center and low, and tilt angles from 0^o(facing upward) to 120^o (facing 30^o downward). They used the SIMPLER (semi-implicit method for pressure-linked equations revised) algorithm to solve the problem. They found that as the Rayleigh number increases, volume flow rate and Nusselt number increase. In addition, as aperture size increases the Nusselt number increases. On the other hand, there was found a nonlinear relation between Nusselt number and inclination angle. They also found that Nusselt number is maximum at the tilt angle of $\varphi = 30^o - 60^o$ for low Rayleigh number and at the tilt angle of $\varphi = 60^o - 90^o$ for high Rayleigh numbers. Hinojosa [6] investigated the numerical results of heat transfer of natural convection of a 2D partially open tilted cavity by illustrating its temperature profiles and flow patterns. The wall facing the opening of the cavity has a constant temperature and other walls are from insulated material. The flow is laminar, 2D, and Boussinesq approach was used for the density of the fluid. For the time discretization, the fully implicit scheme was used. SIMPLEC algorithm was used to

solve the conservation of equations. In addition, SMART scheme was used for the discretization of the convective terms. The fluid Prandtl number is 0.71. The greatest Nusselt number difference for partially open cavity and fully open cavity occur at Ra= 10^8 and φ= 135^o by 55,4 % and the smallest difference occurs at Ra= 10^6 and φ= 90^o by 4.6 %, and the average difference calculated was 29 %.

- **A 2D square open cavity with slots**

Bilgen and Muftuoglu [7] investigated the natural heat transfer in a square open cavity with slots. The wall facing the slots has a constant temperature heating by a uniform heat flux. The changing parameters they studied was the Rayleigh numbers from 10^3 to 10^6, number of slots from 2 to 8 and the dimensionless opening ratio from 0.1 to 0.6. They used finite difference- control volume numerical method to solve the conservation of equations. They found that as Rayleigh number increases the Nusselt number and the volume flow rate increases and on the other hand as the number of slots increases they decreases**.**

- **Open cavities with different shapes**

Prakash et al. [8] analysed the natural convection heat transfer of open cavities with different shapes such as, cubical, spherical and hemispherical geometries having the equal transfer area. They used Fluent software to model and analyse the 3D cavity models. The walls of the cavity are made from copper and the fluid is air. For the low wall temperatures such as equal to 100 ^oC, the Boussinesq approximation was used and laminar model was used. On the other hand, for the higher wall temperatures, k-ε turbulence model, ideal gas characteristics was used for fluid. SIMPLE scheme was used to solve the conservation of equations. The changing parameters for this study were isothermal wall temperatures of 100 ^oC, 200 ^oC and 300 ^oC and opening ratios of 1, 0.5, and 0.25, and also five inclination angles 0^o (aperture facing sideways), 30^o, 45^o, 60^o, and 90^o (aperture facing vertically downwards). They found that increasing the opening ratio increases the convection loss. They observed that natural loss increases when increasing the opening ratio from 0.5 to 1 for both cubical and spherical shapes. Also increasing cavity wall temperature increases the natural convection loss. They observed a decrease in the convection loss when increasing the inclination angle. The highest convection loss was observed at 0^o, while lowest one observed at 90^o. They found that hemispherical cavity has the higher convective loss

when compared with cubical and spherical cavities at opening ratios of 0.5 and 0.25. The spherical cavity was found to have the higher convective loss than the cubical cavity at the opening ratio of 1.

Parakash [9] studied the natural convection heat losses occurring from cubical open cavities in which back wall has a constant higher temperature between 35 ^{o}C and 100 ^{o}C. The cubical cavity has opening ratio of 1. The cavity inclination effect on convective heat loss was studied by using different inclination angles such as 0^{o} (cavity facing sideways), 30^{o}, 45^{o}, 60^{o}, and 90^{o} (cavity facing vertically downwards). The other changing parameter Prakash studied is Rayleigh number changing from 4.5×10^{5} to 1.5×10^{9}. To solve the 3D cubical open cavity model, Parakash used the Fluent CFD software. As increasing the back wall temperature facing to opening, the natural convection heat losses increases. On the other hand, they found that, increasing the inclination angle decreases the natural convection. The highest convection losses were observed at 0^{o} of inclination angle whereas the lowest convection losses were observed at 90^{o}. In addition, this result was analysed for all dimension of cubical cavities. Prakash et al. [10] studied the convective heat losses occurring from downward facing cylindrical cavity receiver. They carried out both test and numerical simulations. The results show that as mean receiver temperature increases, the convective loss increases on the other hand as receiver inclination increases convective loss increases again. They carried out both no-wind tests and external wind tests and at the result they found that convective losses for induced wind is higher than no –wind condition.

- **Nanofluid in open cavity**

Bondareva et al. [11] studied the natural convection of an alumina-water nanofluid in a partially open rectangular cavity with a left conducting solid wall of finite thickness at constant higher temperature and adiabatic top and bottom walls and opening at right side. The single phase nano-fluid model conservation of equations was solved by finite difference method with the given boundary conditions below. The flow was assumed to be laminar, 2D, and satisfy Boussinesq approximation. The viscous dissipation and Joule heating were neglected. Slip effects between the fluid phase and nanoparticles were neglected. The changing parameters of the analysis were Rayleigh number (10^{3} - 10^{6}), thermal conductivity ratio ($1 \leq K \leq 20$), solid wall thickness ($0.1 \leq \delta \leq 0.3$) and the nanoparticles volume fraction ($0 \leq \varphi \leq 0.05$). They

found that increasing the nanoparticles volume fraction in an effective thermal conductivity ratio and dynamic viscosity would lead to decrease in the heat transfer of natural convection and fluid flow rate.

- **Porous media in open cavity**

Hossain et al. [12] studied the unsteady natural convection flow in an open-ended rectangular cavity with the two permeable horizontal surfaces, which were maintained at ambient temperature. They have investigated the effects of buoyancy force and permeability of surfaces on the flow and heat transfer. To solve the governing boundary layer equations, they have used an upwind finite difference method along with the successive over- relaxation iteration technique. They have found that increasing the Rayleigh number increases the heat transfer from the heated surface. The heat transfer decreases from left vertical surface at the region near the bottom surface and it increases in the upper surface. The heat transfer is higher for blowing of fluid than withdrawn fluid from the permeable surfaces and this difference increases with larger Rayleigh numbers.

Combined natural convection and surface radiation in a 2D open cavity

- **A fully open square cavity**

Gonzalez et al. [13] studied the heat transfer of natural convection and thermal radiation on a solar open cavity-type receiver both theoretically and experimentally. The laminar natural convection and surface thermal radiation on the square open cavity at one end were investigated. The theoretical study was carried out on a 2D square open cavity; on the other hand, the experimental study was carried out on an open cavity of cubic shape as a receiver of a solar furnace. The finite volume method and SIMPLEC algorithm was used to solve the conservation of equations. They solved the problem firstly taking the fluid properties as temperature dependent and then at the second case, they took all fluid properties as constant except density, which is the buoyancy term, and Boussinesq approach was used. The changing parameter used was Rayleigh number from 10^4 to 10^6. The other parameter investigated was temperature difference changing from 10 to 400 K and represented as a dimensionless temperature difference (φ). Both theoretical and experimental air temperatures were compared with each other and the deviation was found to be around 3 %.

- **The large temperature difference effect in a 2D open square cavity**

Gonzalez et al. [14] studied the natural convection and surface thermal radiation in a 2D square open cavity receiver for large temperature difference changing from 100 K to 400K and for variable fluid properties. The numerical analysis was repeated for the Rayleigh numbers changing from 10^4 to 10^6. The wall facing the opening has a constant temperature while coming fluid has an ambient temperature of 300 K. On the other hand, top and bottom walls were adiabatic. The fluid was assumed Newtonian and ideal gas and it is air at atmospheric pressure. The fluid flow was assumed laminar and steady state. They used a staggered grid to calculate the velocity components and used a non-staggered grid to calculate the temperature and pressure. The power-law scheme was used for interpolation of the convective terms, while centered- difference scheme was used for interpolation of the diffusive terms. The SIMPLEC algorithm was used to solve the conservation of equations. They found that total average Nusselt number increases as temperature difference increases for the Rayleigh numbers 10^4 and 10^6. In addition, they found that as temperature difference increases radiative heat transfer becomes dominant.

- **A tilted 2D open cavity**

Singh et al. [15] studied a steady, incompressible, laminar flow for combined natural convection with the surface radiation heat transfer in a tilted 2D open cavity in which the wall facing the opening has a constant temperature higher than ambient temperature. They calculated radiation heat transfer by formula of the radiosity-irradiation and for calculating the view factors; they used Hottel's Crossed- string method. They investigated the effects of emissivity, tilt angle and Rayleigh number on the heat transfer in the tilted open cavity. They found that increasing the inclination angle firstly increases the heat transfer but then heat transfer decreases with decreasing the cavity tilt angle for all Rayleigh number and emissivity. They found that the best possible orientation is for the tilt angle of $\varphi = 60^o$, and they found it worse at the tilt angle of $\varphi = 150^o$- 180^o. They also found that surface radiation affects the flow patterns and so that natural convection heat transfer decreases. Hinojosa et al. [16] investigated the natural convection and surface thermal radiation in a tilted 2D open cavity. To design an optimum thermal receiver is very important for the solar concentrators. Since the receiver rotates to collect solar light, the dynamic of the fluid and heat transfer inside the tilted cavity changes. The wall

facing the opening of the cavity has a constant temperature of 500 K whereas incoming fluid has a temperature of 300 K. The other walls are from insulated material. The changing parameters are Rayleigh number from 10^4 to 10^7 and the inclination angle from 0^o to 180^o. The flow is laminar, steady state, and fluid properties are constant except density was chosen as buoyancy term and Boussinesq approximation was assumed. The fluid was assumed non-participating to the radiation and emissivity of the cavity walls are taken as 1. The SIMPLEC algorithm was used for solving conservation of equations. They found that increasing the Rayleigh number, Nusselt number increases except for the inclination angle of 180^o, at which Nusselt number stays constant. Natural convection Nusselt number changes with inclination angle whereas radiative Nusselt number stays constant. The fluid studied has the Prandtl number of 0.71.

- **A tilted 2D porous open cavity**

Milani et al. [17] studied the heat transfer effect of natural convection along with surface radiation in an inclined porous solar cavity by using the means of response surface methodology (RSM). They used Finite Volume Method for discretization and solved the problem with Fluent. They investigated the effects of Rayleigh number ($10^4 \leq Ra \leq 10^6$), Darcy number ($10^{-5} \leq Da \leq 10^3$), inclination angles ($0^o \leq \Theta \leq 90^o$), dimensionless porous substrate thickness ($1/3 \leq \delta \leq 1$), wall surface emissivity ($0 \leq \varepsilon \leq 1$) and surface radiation heat transfer. The sensitivity analysis for Nusselt number depending on those parameters was performed. It was found that Nusselt number increases by increasing Rayleigh number, Darcy number and inclination angle θ. On the other hand, the Nusselt number of natural convection heat transfer decreases as the porous substrate thickness δ increase. They also found out from the sensitivity of Nusselt number on those parameter effects that mean Nusselt number of natural convection is higher than the mean Nusselt number of radiation heat transfer. Hathaway et al. [18] studied the ray tracing impact effect by modeling with Monte Carlo method for performance of a cylindrical solar cavity with a convective boundary. They found that as cavity size increases absorption efficiency increases and wall temperature decreases.

2. MATHEMATICAL MODEL

The schematic of a 2D tilted open square cavity with a uniform heat flux on the left wall and the boundary conditions are given in Figure 2.4. The top and bottom walls of the cavity are adiabatic but the left wall of the cavity is heated constantly by a heat flux, q", and the air comes through the opening wall. The fluid is Newtonian, incompressible, and fluid has constant properties but for the density, Boussinesq approximation was applied. The flow is 2D, laminar, and steady. There is no slip condition on the walls of the cavity. For the solar cavity receiver, the hot wall is made from copper and adiabatic walls are made from wood materials. When surface radiation was taken into account for heat transfer analysis, the emissivity of those materials was used. H is the height and L is the width of square cavity, and since it is a square cavity, H=L.

2.1 Formulations for Natural Convection

The natural, or free, convection is observed as a result of the fluid motion induced by buoyancy forces. The buoyancy force makes the fluid motion because of the density difference results from the temperature difference in the system. Fluid can move downward or upward depending on the heat transfer direction. The natural convection theory explained here by illustrating a fluid motion on a hot vertical wall in the Figure 2.1. As seen from the Figure 2.1, since the left wall is heated, the fluid density decreases near this wall, and an upward fluid motion occurs because of the buoyancy force, and a pressure difference occurs because of the weight of the fluid column. In addition, a thermal and velocity boundary layer forms near the hot wall.
The pressure gradient along the y-axis in the quiescent region becomes:

$$\frac{dp_\infty}{dy} = -\rho_\infty g \tag{2.1}$$

$\frac{dp_\infty}{dy}$: This is the free stream pressure gradient in the quiescent region outside

Quiescent means that fluid is motionless at locations far from the source of buoyancy. On the other hand, near the hot wall, the pressure gradient is:

$$\frac{dp}{dy} = -\rho g \tag{2.2}$$

So that, the net buoyancy force becomes equals to the pressure gradient difference between cold and hot region, and so that subtracting equation 2.1 from equation 2.2, the buoyancy force becomes:

$$K = K(x,y) = g\,(\rho_\infty - \rho) \tag{2.3}$$

The density difference in the natural convection occurs because of the thermal expansion of the fluid. As the fluid gets heated, the density decreases and so that, $\rho_\infty > \rho$. The thermal expansion coefficient expression at constant concentration and pressure is given below:

$$\beta = -\frac{1}{\rho_\infty}\left(\frac{\partial \rho}{\partial T}\right), \quad (K^{-1}) \tag{2.4}$$

In addition, by writing the expansion of this formula we get:

$$\beta = -\frac{1}{\rho_\infty}\ \frac{\rho - \rho_\infty}{T - T_\infty}$$

$$\rho - \rho_\infty = -\rho_\infty \beta\,(T - T_\infty)$$

Buoyancy force K becomes like that:

$$\mathrm{K} = \mathrm{K(x,y)} = \mathrm{g}\,\rho_\infty \beta\,(T - T_\infty) \tag{2.5}$$

The general **momentum** equation is:

$$\rho \frac{DV}{Dt} = -\nabla p + \mu \nabla^2 V$$

Where:

V= V (u, v) in 2D flow

$\frac{DV}{Dt}$: *is the material derivative of* V

$$\frac{D(\ )}{Dt} = \frac{\partial(\ )}{\partial t} + u\frac{\partial(\ )}{\partial x} + v\frac{\partial(\ )}{\partial y}$$

$$\frac{DV}{Dt} = \frac{\partial V}{\partial t} + (V.\nabla)(V)$$

$$\nabla(\ ) = \frac{\partial(\ )}{\partial x}\hat{\imath} + \frac{\partial(\ )}{\partial y}\hat{\jmath}$$

$$V.\nabla(\ ) = u\frac{\partial(\ )}{\partial x} + v\frac{\partial(\ )}{\partial y}$$

Since the fluid motion along the hot vertical wall is upward, and the gravity direction is downward, so body force due to gravity effect is added to the momentum equation with minus sign as below:

$$\rho \frac{DV}{Dt} = -\nabla p + \mu \nabla^2 V - \rho g \tag{2.6}$$

Therefore, the momentum equation above for the quiescent fluid is like that:

$$0 = -\nabla p_\infty - \rho_\infty g \tag{2.7}$$

Then, subtracting the equation 2.7 from the equation 2.6, the momentum equation for the natural convection becomes:

$$\rho \frac{DV}{Dt} = -\nabla (p - p_\infty) + \mu \nabla^2 V - g(\rho - \rho_\infty) \tag{2.8}$$

According to the Oberbeck-Boussinesq approximation, the fluid density in the all terms except Buoyancy force in the momentum equation was assumed constant and equal to the ρ_∞. So that, **the final form of the momentum equation** for the natural convection becomes like that [19]:

$$\rho_\infty \frac{DV}{Dt} = -\nabla p + \mu \nabla^2 V + \mathrm{g}\, \rho_\infty \beta\, (T - T_\infty) \tag{2.9}$$

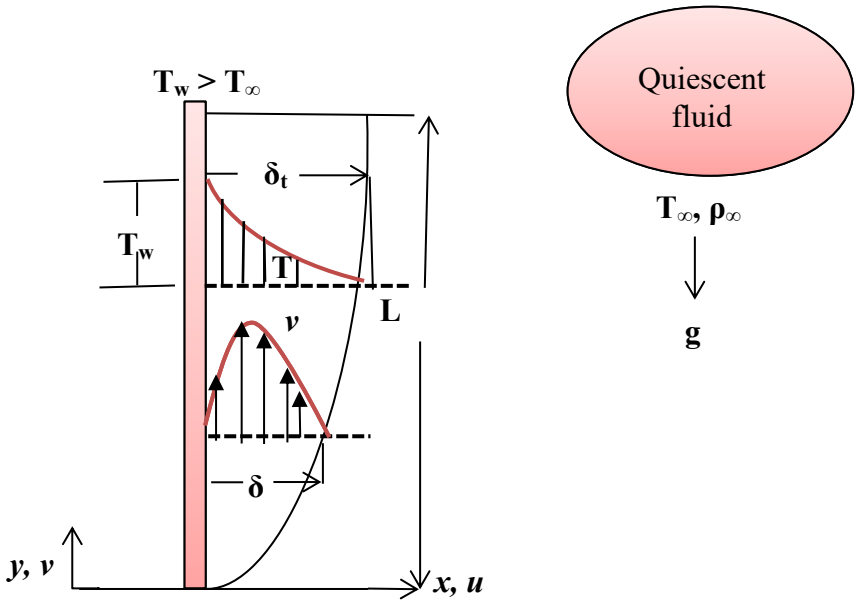

Figure 2. 1 : Natural convection boundary layer development on the hot wall.

The conservations of equations for natural convection in a tilted open cavity

The fluid flow is 2D, laminar, and fluid is incompressible and flow is at the steady state. Boussinesq approximation was used for the fluid density. The conservation of

equations for continuity, momentum and energy in the dimensional form are as follows:

Continuity equation:

$$\frac{\partial u}{\partial x}+\frac{\partial v}{\partial y}=0 \tag{2.10}$$

Momentum equation:

x- direction:

$$\frac{\partial(\rho_\infty u^2)}{\partial x}+\frac{\partial(\rho_\infty uv)}{\partial y}=-\frac{\partial p}{\partial x}+\mu\left(\frac{\partial^2 u}{\partial x^2}+\frac{\partial^2 u}{\partial y^2}\right)+g\rho_\infty\beta(T-T_\infty)cos\varphi \tag{2.11}$$

y- direction:

$$\frac{\partial(\rho_\infty uv)}{\partial x}+\frac{\partial(\rho_\infty v^2)}{\partial y}=-\frac{\partial p}{\partial y}+\mu\left(\frac{\partial^2 v}{\partial x^2}+\frac{\partial^2 v}{\partial y^2}\right)+g\rho_\infty\beta(T-T_\infty)sin\varphi \tag{2.12}$$

Energy equation:

$$u\frac{\partial T}{\partial x}+v\frac{\partial T}{\partial y}=\alpha\left(\frac{\partial^2 T}{\partial x^2}+\frac{\partial^2 T}{\partial y^2}\right) \tag{2.13}$$

In this study, Rayleigh number changes with gravity. The value of Rayleigh number gives laminar flow conditions ($Ra_L < 10^9$).

Rayleigh number can be computed from: $Ra=\frac{g\beta\Delta TL^3}{\alpha\nu}$

The physical properties of air are defined in accordance with ambient temperature, and characteristic length L is taken as the width of square cavity. Prandtl number for the fluid in this thesis study can be computed from:

$$Pr=\frac{\nu}{\alpha}=0{,}717$$

The local convective Nusselt number (Nu_x) calculations:

At the stagnant region formed in the interface of the solid and fluid, the conduction heat transfer is equal to the convection heat transfer [19]:

$$q''_{cond}=q''_{conv} \tag{2.14}$$

$$-k\left(\frac{\partial T}{\partial x}\right)_{wall} = h\,(T_H - T_\infty) \tag{2.15}$$

$$\mathrm{h} = -\mathrm{k}\left(\frac{\partial T}{\partial x}\right)_{wall} * \frac{1}{(T_H - T_\infty)} \tag{2.16}$$

The minus sign in the conduction heat transfer indicates that temperature gradient has a negative slope, which means that temperature is decreasing from hot wall to the right opening wall. The direction of heat transfer is from hot wall to the opening wall. Then, local Nusselt number (Nu_x) changing along the x- axis can be calculated by the formula:

$$\mathrm{Nu}_x = \frac{q_{conv}''}{q_{cond}''} = \frac{\mathrm{hx}}{\mathrm{k}} = -\left(\frac{\partial T}{\partial x}\right)_{wall} * \frac{x}{(T_H - T_\infty)} \tag{2.17}$$

The average convective Nusselt number ($\overline{Nu_c}$) calculations:

The energy balance of convection and conduction in the equation 2.15, above for the left wall can be written again and when integrating the both side of the equation with respect to y-axis, average Nusselt number for the left wall can be found and it can be also found for the right wall for the closed cavity.

$$\int_0^L \mathrm{h}\,(T_H - T_\infty)\,dy = \int_0^L -\mathrm{k}\left(\frac{\partial T}{\partial x}\right)_{wall} dy \tag{2.18}$$

$$\overline{Nu_c} = \frac{hL}{k} = \int_0^L -\left(\frac{\partial T}{\partial x}\right)_{wall} \frac{1}{(T_H - T_\infty)}\,dy \tag{2.19}$$

Since, $\dfrac{q_{cond}''}{k} = -\left(\dfrac{\partial T}{\partial x}\right)_{wall}$

$$\overline{Nu_c} = \int_o^L \frac{q_{cond}''}{k}\left(\frac{1}{T_H - T_\infty}\right)dy = \frac{q_{\mathrm{cond}''}}{k}\frac{L}{\Delta T} \tag{2.20}$$

In Ansys Fluent, total heat flux on the wall can be taken to calculate the average Nusselt number by using the equation 2.20.

2.2 Formulations for Surface to Surface Radiation

In this study, the fluid was not participating to the radiation so that just a surface-to-surface (S2S) radiation exists. To calculate surface radiation and net radiative heat flux over the walls of cavity, walls are divided into parts depending on the mesh used. The parameters affect the S2S radiation are the size of the cavity, orientation of the cavity and separation distance between two surfaces. To calculate the effects of these parameters by using view factor model, **the view factors** are calculated. The radiation heat flux for a surface consists of directly emitted energy and reflected energy. The reflected energy flux is affected by the incident energy flux from the surroundings. When radiant energy strikes a material surface, part of it is reflected, part is absorbed and part is transmitted. **P** is the fraction reflected and is defined as reflectivity, **α** is the absorptivity as the fraction absorbed and **τ** is the transmissivity as the fraction transmitted. The formula for the relation between these three terms is:

$$\rho + \alpha + \tau = 1 \tag{2.21}$$

The transmissivity is neglected because most of the solid bodies as in the solar cavity materials do not transmit the thermal radiation. So the above formula becomes:

$$\rho + \alpha = 1 \tag{2.22}$$

The emissivity (ε) is equal to the absorptivity (α) for a blackbody. A = ε and so that,

$$\rho = 1 - \varepsilon_i \tag{2.23}$$

$$E_{bi} = \sigma T_i^4 \quad (W/m2) \tag{2.24}$$

Where:

E_{bi} : is the total energy (W/m^2) emitted and is proportional to the absolute temperature (K) to the fourth power at surface I and the above equation is called the Stefan- Boltzmann law, E_b is the energy radiated per unit time and per unit area by the ideal radiator.

σ: is called the Stefan- Boltzmann constant, which has the value

σ= 5.669 x 10^{-8} W/m^2 K^4. The Figure 2.2, given below shows the radiation exchange between two surfaces.

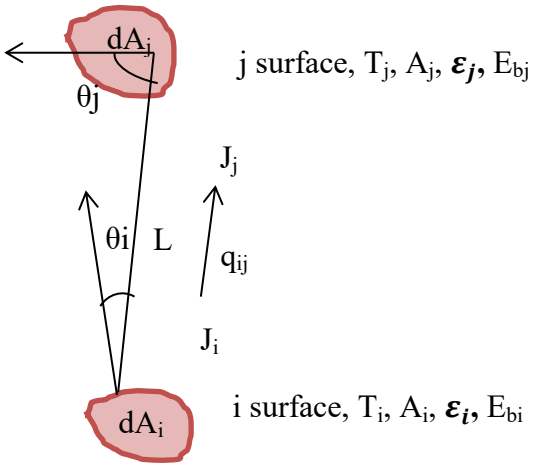

Figure 2. 2 : The radiation exchange between two surfaces.

Here:

F_{ij} is the radiation view factor and it is a fraction of energy leaving a surface I that reaches surface j. A_i and A_j are the surface areas of I and j surfaces respectively.

L is the line distance that connects dA_i and dA_j surfaces and θ_i and θ_j are the angles between the normals of the surfaces. The view factors can be calculated by the following expression [23]:

$$F_{ij} = \frac{1}{A_i} \iint_{A_j A_i} \frac{\cos\theta_i \cos\theta_j}{\pi L^2} dA_i dA_j \tag{2.25}$$

$$F_{ji} = \frac{1}{A_j} \iint_{A_j A_i} \frac{\cos\theta_i \cos\theta_j}{\pi L^2} dA_i dA_j \tag{2.26}$$

The properties of the view factors are those [23]:

- There is a reciprocity relation between view factors and surface areas:

$$A_i F_{ij} = A_j F_{ji} \tag{2.27}$$

- The summation rule for the view factor is:

$$\sum_{j=1}^{N} F_{ij} = 1 \tag{2.28}$$

Here, N is the total number of parts along the cavity surface. Such as F_{11} +F_{12}+F_{13}= 1.0, whereas F_{11}=F_{22}=F_{33}= 0, (F_{ii}= 0). F_{11} represents the fraction of energy leaving surface 1 that strikes surface 1.

- There is a superposition rule between view factors given below [25]:

$$F_{1\to(2,3)} = F_{1\to2} + F_{1\to3} \tag{2.29}$$

- If surfaces j and k are symmetric about the surface I then there is a symmetry rule for view factors:

$$F_{i\to j} = F_{i\to k} \tag{2.30}$$

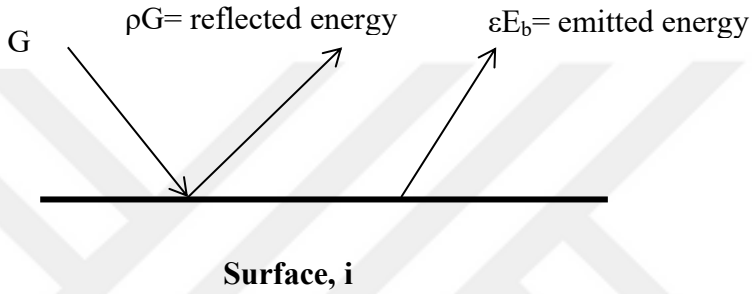

Figure 2. 3 : Incident, reflected and emitted heat transfer on a surface i, with emissivity ε.

G = irradiation = total radiation incident upon a surface per unit time and per unit area.

J = radiosity = total radiation that leaves a surface per unit time and per unit area.

The radiosity is the sum of the energy emitted and the energy reflected when no energy is transmitted, or

$$J_i = \varepsilon_i E_{bi} + \rho_i G_i \tag{2.31}$$

Here, ε is the emissivity and substituting the equation 2.23 into the equation 2.31, J_i becomes equal to the equation below [25]:

$$J_i = \varepsilon_i E_{bi} + (1 - \varepsilon_i) G_i \qquad (W/m2) \tag{2.32}$$

Here from this equation, we get:

$$G_i = \frac{J_i - \varepsilon_i E_{bi}}{1 - \varepsilon_i} \tag{2.33}$$

The net energy leaving the surface I, is the difference between the radiosity and the irradiation, equal to J – G.

$$The\ net\ radiative\ heat\ transfer\ =\ \frac{q_i}{A_i} = J_i - G_i, \qquad (W/m^2) \quad (2.34)$$

Substituting G_i, in the equation 2.33, into the equation 2.34:

$$q_i\ = A_i \left(J_i - \frac{J_i - \varepsilon_i E_{bi}}{1 - \varepsilon_i}\right), \quad (W) \quad (2.35)$$

Finally, we get net radiative heat transfer for surface i, as [23]:

$$q_i = A_i \varepsilon_i \left(\frac{E_{bi} - J_i}{1 - \varepsilon_i}\right) \quad (2.36)$$

The direction of the net heat transfer depends on the size of the energy of the J_i and E_{bi}, and if:

$E_{bi} > J_i$, heat flow is from the surface i.

$J_i > E_{bi}$, heat flow is towards the surface i.

In other words, if q_i is negative, direction of heat transfer is towards the surface i.

The net radiative heat transfer between any two surfaces [24]:

The irradiation G_i, comes to i surface is:

$$A_i G_i = \sum_{j=1}^{N} A_j F_{ji} J_j \quad (2.37)$$

Since $A_i F_{ij} = A_j F_{ji,}$ the above equation 2.37 becomes like that:

$$G_i = \sum_{j=1}^{N} F_{ij} J_j \quad (2.38)$$

The radiosity J_i , leaving the i surface is:

$$J_i = \sum_{j=1}^{N} F_{ij} J_i \quad (2.39)$$

The net radiative heat transfer is:

$$q_i = A_i (J_i - G_i) \quad (2.40)$$

Substituting the J_i and G_i into the equation 2.40:

$$q_{ij} = A_i J_i F_{ij} - A_i J_j F_{ij} \tag{2.41}$$

$$q_{ij} = A_i F_{ij} (J_i - J_j) \tag{2.42}$$

For a number of N surfaces the equation 2.42 becomes equal to:

$$q_i = \sum_{j=1}^{N} q_{ij} = A_i \sum_{j=1}^{N} F_{ij} (J_i - J_j) \tag{2.43}$$

The equation 2.36 is equal to the equation 2.43 and we get E_{bi} from this equality:

$$q_i = A_I \varepsilon_i \left(\frac{E_{bi} - J_i}{1 - \varepsilon_i} \right) = A_i \sum_{j=1}^{N} F_{ij} (J_i - J_j) \tag{2.44}$$

$$E_{bi} = \sigma T_i^4 = J_i + \frac{1 - \varepsilon_i}{\varepsilon_i} \sum_{j=1}^{N} F_{ij} (J_i - J_j) \tag{2.45}$$

The equation 2.44 is for the T_i temperature defined for i surfaces. And by writing the G and E_b equations into the equation 2.31 we get J_i and J_j equations respectively:

$$J_i = \varepsilon_i \sigma T_i^4 + (1 - \varepsilon_i) \sum_{j=1}^{N} F_{ij} J_j \tag{2.46}$$

$$J_j = \varepsilon_j \sigma T_j^4 + (1 - \varepsilon_j) \sum_{i=1}^{N} F_{ij} J_i \tag{2.47}$$

If the surfaces have the blackbodies property then $\varepsilon_i = \varepsilon_j = 1$, and we get:

$J_i = \varepsilon_i \sigma T_i^4$

$J_j = \varepsilon_j \sigma T_j^4$

So that, for blackbodies the net radiative heat transfer for N surfaces becomes equal to the:

$$q_i = \sum_{j=1}^{N} q_{ij} = A_i \sum_{j=1}^{N} F_{ij}(T_i^4 - T_j^4) \quad (for\ blackbodies)$$

The average radiative Nusselt number calculation:

$$\frac{q_i}{A_i} = q_r = is\ the\ net\ radiative\ heat\ flux, (W/m^2) \tag{2.48}$$

$$\overline{Nu_r} = N_r \int_0^1 -Q_r\, dY \tag{2.49}$$

Where:

$$N_r = \frac{\sigma T_H^4 L}{k(T_H - T_\infty)} \tag{2.50}$$

N_r: Dimensionless parameter of conduction radiation

$$Q_r = \frac{q_r}{\sigma T_H^4} \tag{2.51}$$

Q_r: Dimensionless net radiative heat flux on the corresponding adiabatic wall

$$Y = \frac{y}{H} \tag{2.52}$$

The total average Nusselt number can be found by summing of Nusselt numbers of natural convection and surface radiation:

$$\overline{Nu_t} = \overline{Nu_c} + \overline{Nu_r} \tag{2.53}$$

$$\overline{Nu_t} = \int_o^L -\left(\frac{\partial T}{\partial x}\right)_{wall} \left(\frac{1}{T - T_\infty}\right) dy + N_r \int_0^1 -Q_r\, dY \tag{2.54}$$

In ANSYS Fluent, the area weighted average total heat flux on the hot wall can be taken to calculate the total Nusselt number. In addition, the average radiative heat flux can be taken in Fluent.

$$\overline{Nu} = \frac{\bar{q} L}{k \Delta T} \tag{2.55}$$

Where $\bar{q}$ (W/ m^2) is total average heat flux on the hot wall. It can be also found from those formulas, by using hot wall boundary conditions:

$$q_{cond}'' = -k \left(\frac{\partial T}{\partial x}\right)_{wall} = q_{conv}'' = h(T - T_\infty)$$

2.3 The Boundary Conditions

2.3.1 Fully open inclined square cavity:

The boundary conditions of a fully inclined open square cavity system are shown in Figure 2.4 and the boundary conditions of a fully open square cavity system with a tilt angle of 90^o are shown in Figure 2.6-b.

When dimensionless aperture size = h / H= 1, it is called a **fully open cavity**.

The assumptions done for the boundary conditions are those:

- There is no slip on the solid walls.
- The left wall of the open square cavity was heated constantly by a heat source (q") so that it has a constant temperature of T_H.
- In addition, *u*= 0 and *v*= 0 on the left wall and adiabatic walls.
- Since the upper and bottom walls are adiabatic, the temperature gradient is zero on these walls.

$$\frac{\partial T}{\partial y} = 0$$

On the other hand, when radiation exists it becomes to equal to:

$$-k\left(\frac{\partial T}{\partial y}\right)_{y=0,L} = q_r$$

Where:

q_r is the net radiative heat flux (W/m^2)on the adiabatic walls.

- The air coming from opening has a fixed ambient temperature of T_∞. The outgoing fluid temperature gradient is zero due to greater effect of the convection heat transfer on the conduction heat transfer.
- At the opening wall, the derivative of the velocity component is zero because the fluid velocity profile does not change in this direction (V in x direction).

$$p = 0, \quad \frac{\partial v}{\partial x} = 0, \quad \frac{\partial u}{\partial x} = -\frac{\partial v}{\partial y}, \quad \left(\frac{\partial T}{\partial x}\right)_{out} = 0, \quad T_{in} = T_\infty$$

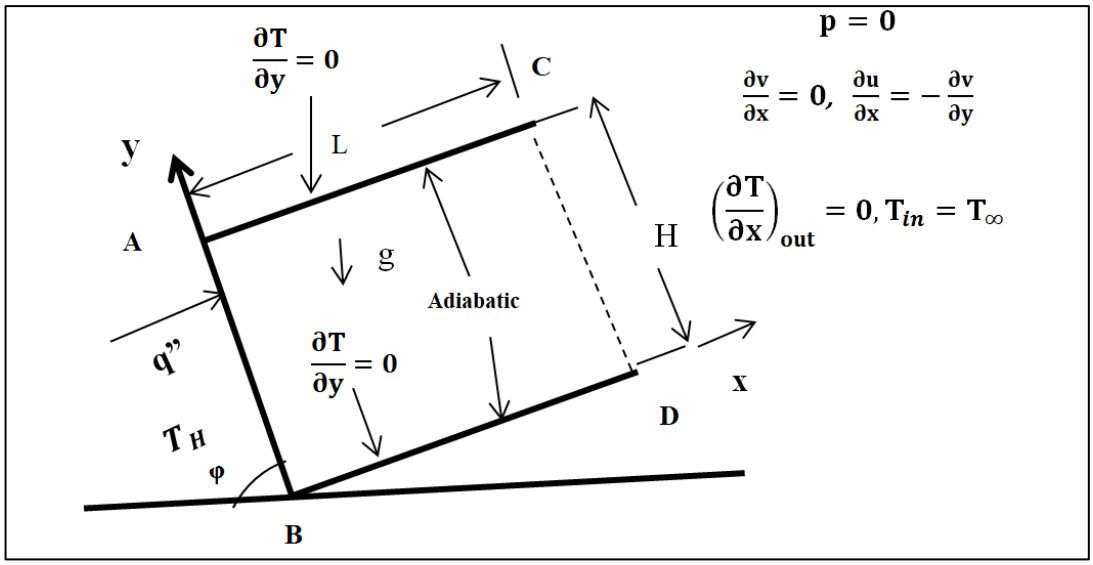

Figure 2. 4 : Schematic of the fully open cavity system, the coordinate system and boundary conditions.

2.3.2 Partially open square cavity:

The difference from above case is just that the cavity is partially open and does not incline. The boundary conditions are all same. The schematic of the partially open cavity system is given in Figure 2.5 below.

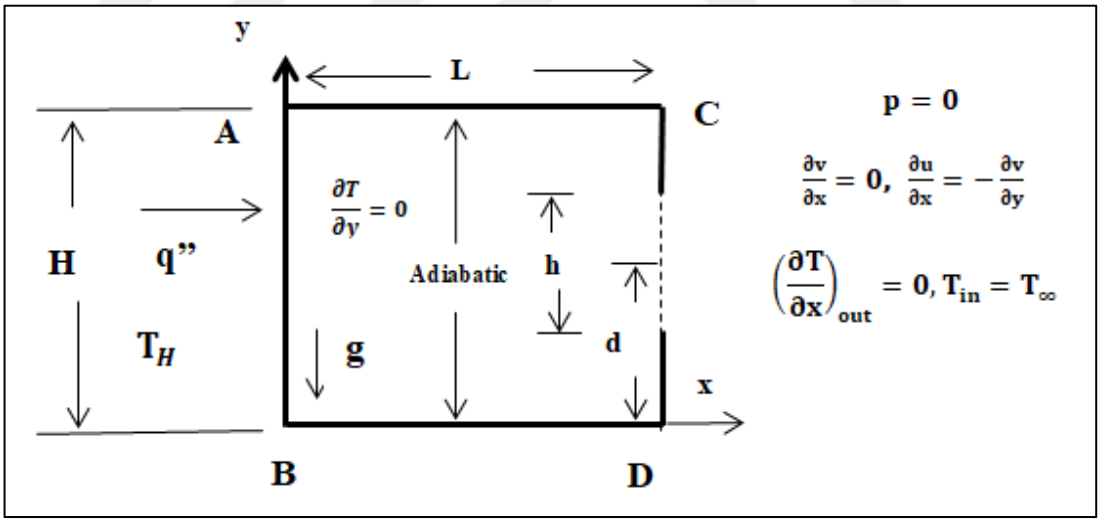

Figure 2. 5 : Schematic of the partially open cavity system, the coordinate system and boundary conditions.

2.3.3 Closed square cavity

The boundary conditions for a closed square cavity differs from an open cavity by taking the boundary condition of right wall as a constant cold temperature equal to 300 K. The differences of open and closed square cavity schematic system are given

in Figure 2.6. The fluid flow is again 2D, laminar, incompressible, and steady and Boussinesq approach was applied for density.

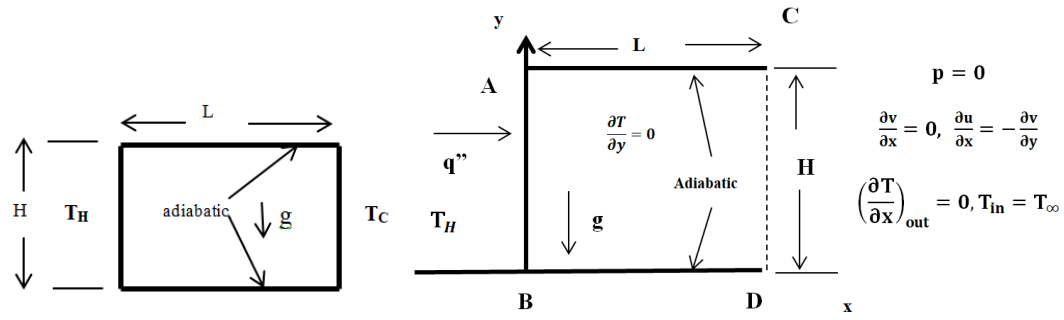

a) Closed Cavity **b) Open Cavity**

Figure 2. 6 : Schematic of the a) closed cavity and b) open cavity system, the coordinate system and boundary conditions**.**

3. NUMERICAL METHOD

Ansys Fluent software was used to model a laminar and steady state flow, both pure natural convection and combined pure natural convection and surface radiation heat transfer in the 2D square cavity and simulate the results and to calculate the Nusselt number. The conservation of equations from (1) to (4) was solved by using SIMPLE (Semi-implicit method for pressure linked equations) Algorithm. Pressure based solver was used. Second Order Upwind method was used for both Momentum and Energy. Boussinesq approximation was applied to the density of the fluid. The boundary conditions of the opening wall of the cavity defined as pressure inlet. The boundary condition for the hot wall was defined as Temperature and for the insulated wall heat flux = 0 W/m^2 was defined. In this study, “surface-to-surface" radiation needs to be considered for analysis.

The Surface-to-Surface (S2S) radiation model [21], which assumes that all surfaces are gray and diffuse, was used to compute the radiation heat transfer in a solar cavity receiver. The heat transfer between two surfaces depends in part on their size, separation distance, and orientation. These parameters are calculated by a geometric function called a “view factor". If a certain amount of radiation is incident on a graybody model surface, then a fraction is reflected, a fraction is absorbed, and a fraction is transmitted. The S2S model assumes that any absorption, emission, or scattering of radiation by the medium can be ignored. In solar cavity receiver the cavity wall surfaces was considered opaque. The emissivity is equal to the absorptivity for gray, diffuse, and opaque surfaces and that reflectivity is equal to 1 minus the emissivity. When the S2S model was used, the interior fluid was assumed non-participating medium and this provides the main advantage of this option to speed up the view factor calculation and the radiosity calculation. The convergence criterion for the continuity and momentum residuals was taken as 10^{-3}, and for the energy residual was taken as 10^{-6}. Solution procedure summary for pure natural convection thermal analysis in closed cavity was given in Table A.1, and in open

cavity, it was given in Table A.2. Also the combined pure natural convection and surface radiation solution procedure was given in Table A.3.

4. RESULTS AND DISCUSSIONS

4.1 Mesh Grid Indepence Test

In order to get the correct solution from analysis a mesh grid test was applied for Ra= 10^6 case. The mean Nusselt number for hot wall under constant heat flux was considered to evaluate the independence of the grid. The result of the mean Nusselt numbers for different number of grids was given in Table 4.1. As seen from the mesh grid test results, there was % 0,5 decrease in Nusselt number between 90 x 90 grid and 100 x 100 grid and on the other hand, there was a % 0,20 decrease in Nusselt number between 100 x100 grid and 110 x 110 grid. Since the Nusselt number, does not change anymore after 100x 100 grid,100x 100 grid was selected to solve the equations of conservations. The 2D Mesh model with 100 x 100 grid is given in Figure 4.1. The mesh model settings is given in Table 4.2. Mapped face meshing was used and edge size method was used by selecting four edges of the square cavity and number of division segment was adjusted to give the necessary grids for a square cavity.

Table 4. 1 : The results of the mean Nusselt number.

Number of grids in X–Y	The mean Nusselt number
40 x 40	9,433
50 x 50	9,234
60 x 60	9,101
70 x 70	9,029
80 x 80	8,981
90 x 90	8,948
100 x 100	8,924
110 x 110	8,906
120 x 120	8,893

Mesh Model Used

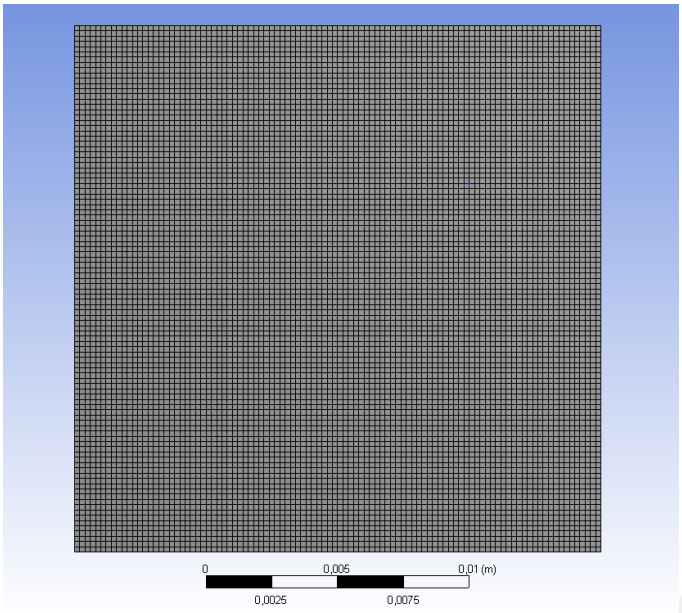

Figure 4. 1 : Mesh model for closed cavity.

Table 4. 2 : Mesh program settings.

Mesh Method	Mapped Face Meshing, Quadrilaterals	
Edge Sizing	4 edges	
Number of Division	100	
Behavior	Hard	
Bias Type	No Bias	
Named Selections		
heated face	hot	
air coming face	cold	
insulated face	ins	
Mesh nodes	10201	
Mesh elements	10000	
Aspect ratio min	1	
Aspect Ratio max	1	
Skewness max	1,31 E-10	<0,98
Orthogonality min	1	>0,1
good	worse	neutral

4.2 Numerical Solution and Validation Studies

In order to validate the mathematical model used, firstly, the closed square cavity problem was solved for $\varphi = 90^{o}$. Nusselt number results and isotherms, streamlines were compared with the published ones. Secondly, pure natural convection thermal analysis was performed for a fully open square cavity for $\varphi = 90^{o}$, and Nusselt number results were compared with the published ones. Thirdly, pure natural convection heat loss in a tilted square open cavity was investigated. Fourthly, pure natural convection analysis for a partially open square cavity for $\varphi = 90^{o}$, was performed and isotherms, streamlines and velocity vector results were compared with Bilgen and Oztop's published results. Then the Nusselt number results were compared with a fully open square cavity. The last two validations were radiative model validation and combined pure natural convection and surface radiation validation in a fully open square cavity and the Nusselt number results comparison with published ones.

4.2.1 Pure natural convection analysis in closed square cavity

Problem definition and discussions: There is a square closed cavity heated from left sidewall and cooled by the right wall and bottom and top walls are adiabatic. The schematic of the closed system is given in Figure 2.6 -a. The pure natural convection for 2D, laminar, incompressible, steady state flow was investigated. The boundary conditions set in Fluent is given in Table A.1 in Appendix A. In this section, the effect of the different Rayleigh numbers on the pure natural convection in a closed cavity was investigated. The Rayleigh number was varied from 10^2 to 10^6. As can be seen from Figure 4.7, the velocity vector result for $Ra=10^5$, the flow direction is clockwise inside the cavity. The isotherms and streamlines for Rayleigh numbers from 10^2 to 10^6 given from Figure 4. 2 to Figure 4.6. The fluid heated by the hot wall moves to the top wall by buoyancy effect and transfers its heat to the cold wall. The insulated wall keeps the heat received by the fluid and behaves as an energy corridor for the fluid flow. As can be seen from isotherms, a thermal boundary layer forms on the hot wall and cold wall. The Figure 4.2 in which isotherms for $Ra=10^2$ was illustrated and as can be seen from this isotherms, conduction heat transfer is dominant and isotherms are uniform. And from left to right in the cavity, temperature decreases. As can be seen from isotherms results as Rayleigh number increases,

thermal boundary layer thickness on the right wall decreases and volume occupied by the cold fluid inside the cavity increases. The isotherms get more close to the left bottom side of the wall and through the top wall; they get away from each other. The temperature gradient is highest at the point where isotherms gets more close to the each other, in other words as the thermal boundary layer of thickness decreases, temperature gradient increases. When we look at the streamlines, as Rayleigh number increases velocity gradient increases on the walls and streamlines gets more close to the walls and the thickness of the velocity boundary layer decreases. On the other hand, as Rayleigh number increases, fluid velocity increases. This means that as Rayleigh number increases natural convection heat transfer increases, and natural convection heat transfer becomes dominant with respect to conduction heat transfer at high Rayleigh numbers. When we look at the streamlines for different Rayleigh numbers, just one cell form for the Rayleigh numbers of 10^2, 10^3 and 10^4 and on the other hand, for Rayleigh numbers of 10^5 and 10^6, there form many cells of stream function. As can be seen from the Table 4.3, the average Nusselt Number Results, the datas are more close to the published ones. So the mathematical model was verified.

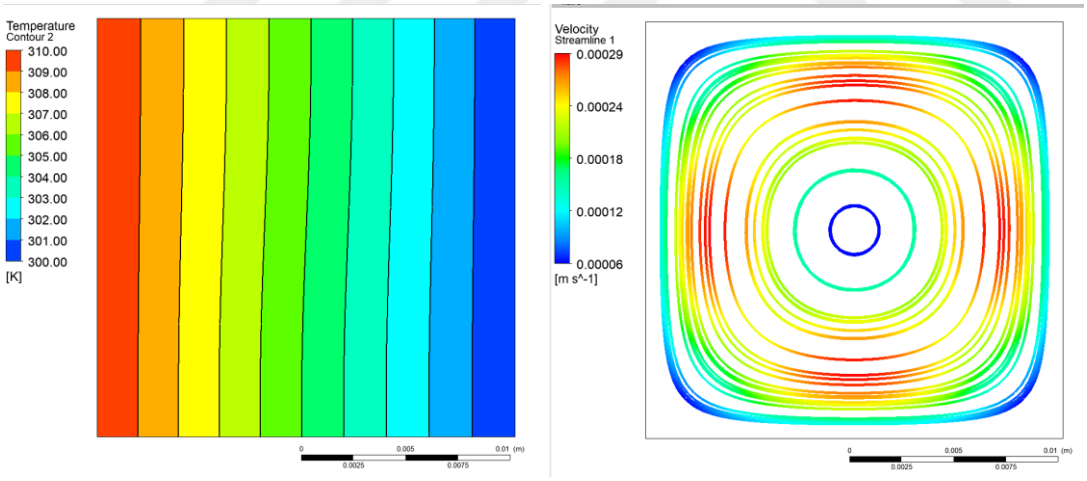

Figure 4. 2 : Isotherms and streamlines from left to right respectively for Ra= 10^2.

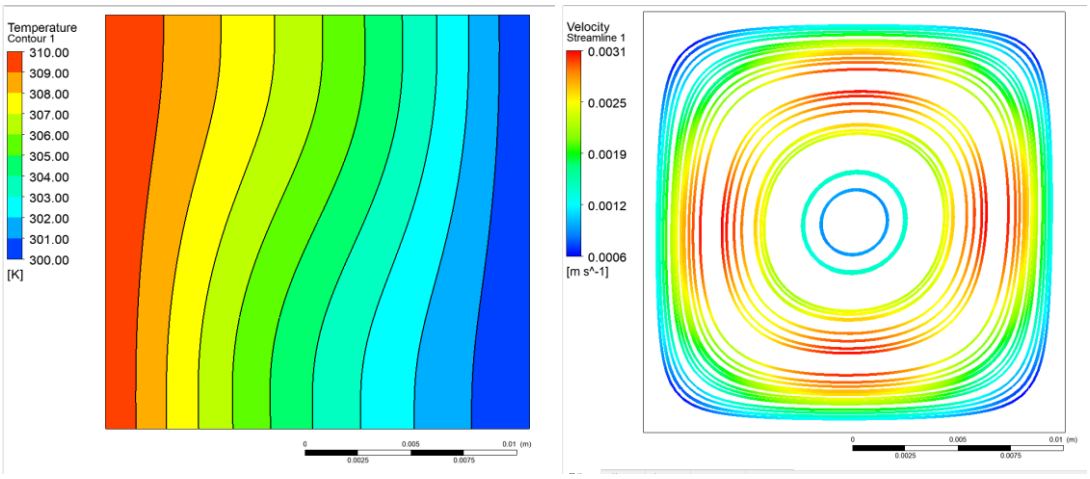

Figure 4. 3 : Isotherms and streamlines from left to right respectively for Ra= 10^3.

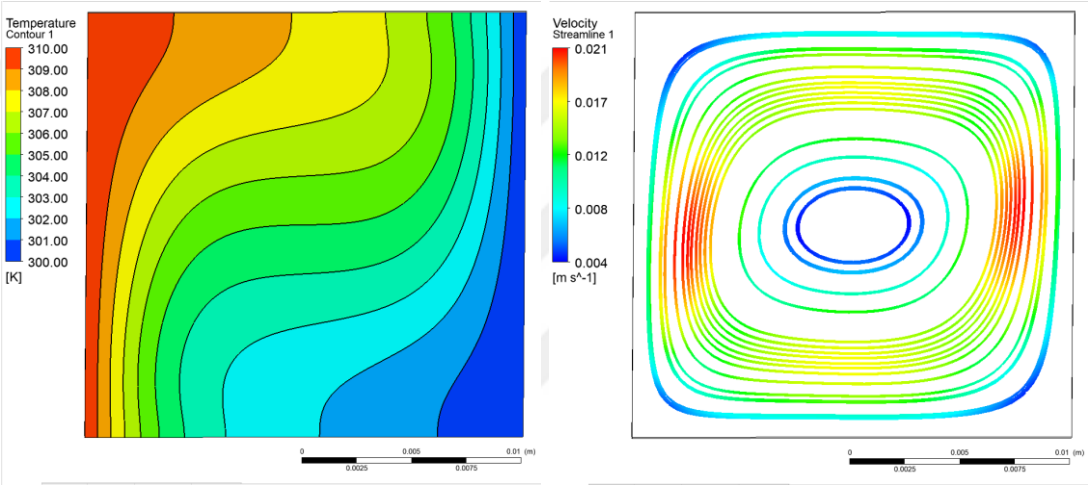

Figure 4. 4 : Isotherms and streamlines from left to right respectively for Ra= 10^4.

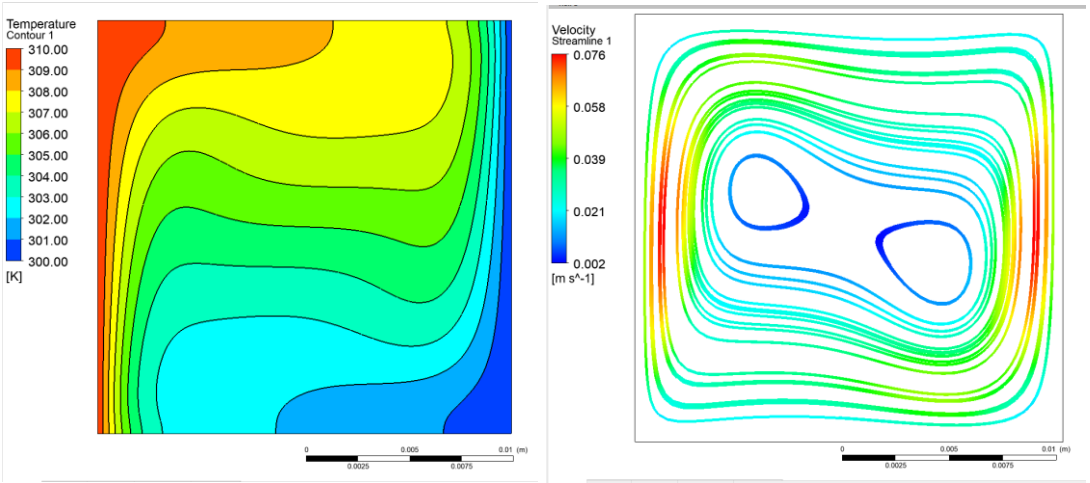

Figure 4. 5 : Isotherms and streamlines from left to right respectively for Ra= 10^5.

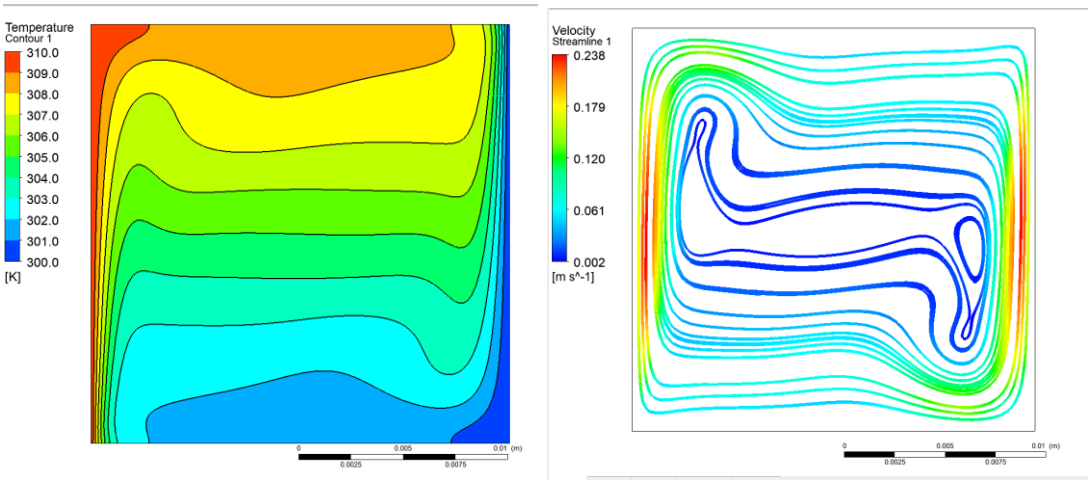

Figure 4. 6 : Isotherms and streamlines from left to right respectively for Ra= 10^6.

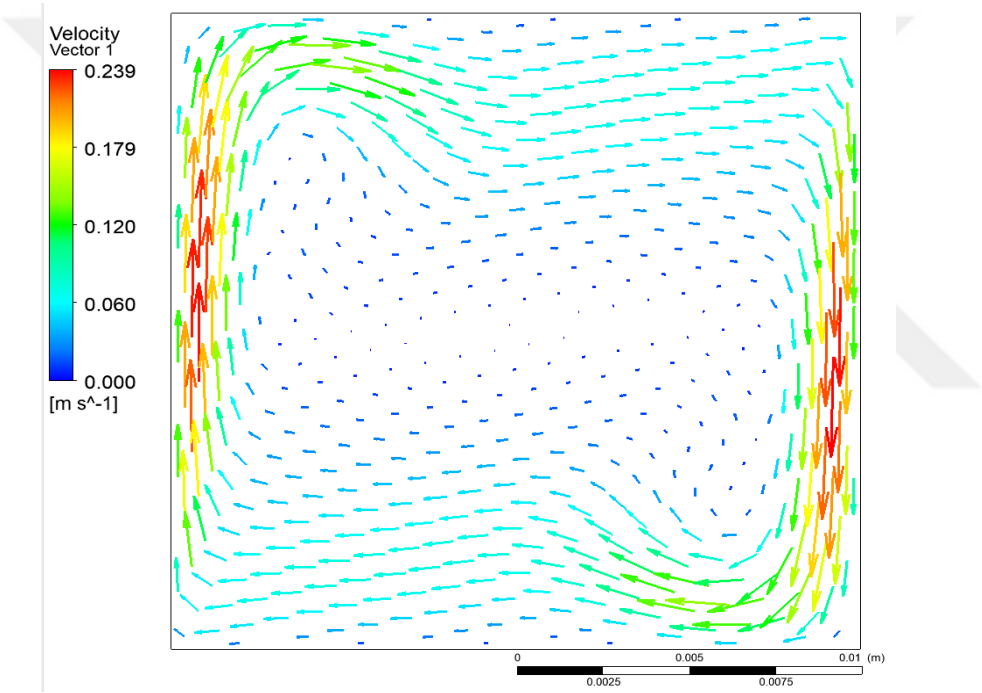

Figure 4. 7 : Velocity vector results for Ra= 10^5.

Table 4. 3 : Nusselt number results for pure natural convection in a closed square cavity.

closed cavity			Average Nusselt numbers for hot wall				
Ra	Gravity, m/s^2	Total heat flux on the hot wall, W/m^2	**present study**	A. C. Baytaş[19]	Elatar et al.[1]	S. Kumar[4]	Bairi A.[2]
10^2	0,13	13,063	**1,001**	1,001			
10^3	1,3	14,032	**1,075**	1,119			1,112
10^4	13	28,602	**2,191**	2,236	2,234	2,188	2,168
10^5	130	59,339	**4,546**	4,504	4,517	4,529	4,228
10^6	1300	116,4899	**8,924**	8,658	8,948	8,823	8,243

4.2.2 Pure natural convection analysis in a fully open square cavity with $\varphi = 90^{o}$.

In order to validate the mathematical model, pure natural convection with Pr=0,71 in a square cavity was solved, ant the results were compared with the published results in Table 4.4.

Problem definition and discussions: The schematic of the fully open square cavity is given in Figure 2.6-b. There is an open square cavity heated from left sidewall with temperature of 310 K and cooled by opening wall with an ambient temperature of 300 K and bottom and top walls are adiabatic. The pure natural convection for a 2D, laminar, incompressible and steady state flow was investigated. The Boussinesq approximation was applied for the density of the fluid. The Rayleigh numbers from 10^2 to 10^6 was taken as the changing parameter of the validation study.

As can be seen from the isotherms of pure natural convection analysis results from Figure 4.8 to Figure 4.12, there forms a thermal boundary layer near the hot wall and as Rayleigh number increases thermal boundary layer and velocity boundary layer thicknesses on the hot wall decreases and the volume occupied by the cold fluid increases. This means that as thermal, velocity boundary layer thicknesses decrease temperature, and velocity gradient increases on the hot wall. In addition, when we look at the pressure contours, pressure decreases from left side through the right side of the top wall. This pressure decreasing creates a fluid flow from left to right. At the same way, pressure decreases from top right corner through the bottom right corner and it decreases from bottom right corner through the left bottom corner. Since from high pressure to low pressure a fluid flow forms, as can be seen clearly in the velocity vector results, a clockwise fluid flow in the open cavity forms. The velocity vector direction is clockwise such as cold fluid enters from bottom, reaches to the hot wall, and gets heated then by buoyancy effect it exits from right side of the top wall with higher velocity. As can be seen from Table 4.4 and Table 4.5, for pure convection heat loss, it does not important what type of material of cavity is made from because this is a 2D thermal analysis and shell conduction was not defined in Fluent so conduction through the walls of the cavity was not taken into account so that all the Nusselt numbers results are same. In addition, the Nusselt numbers found in this study are more close to the published results so the mathematical model was also verified for pure natural convection in a fully open square cavity.

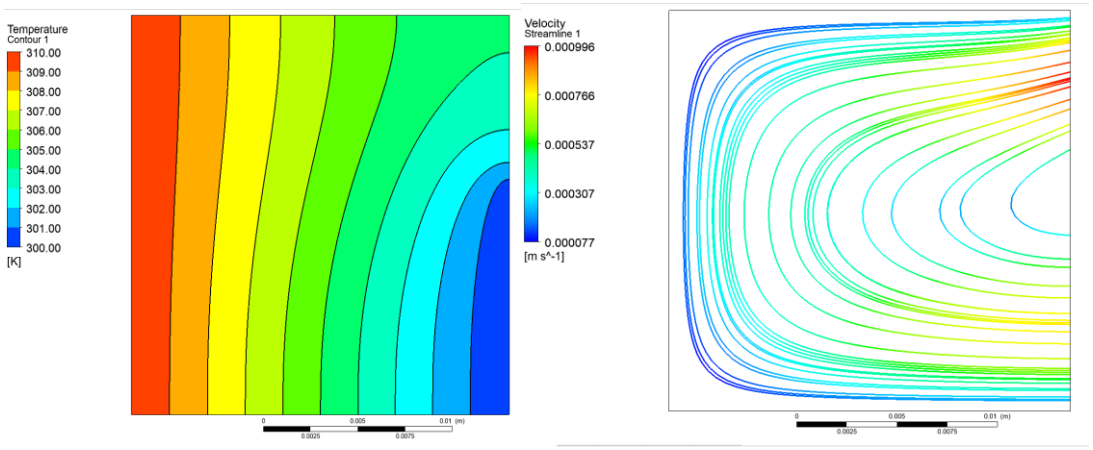

a) b)

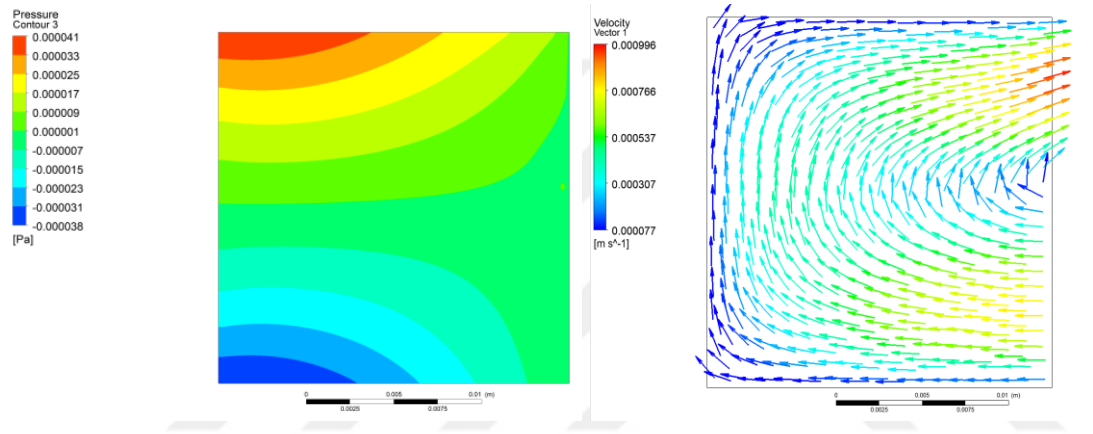

c) d)

Figure 4. 8 : a) Isotherms, b) Streamlines, c) Pressure contours, d) Velocity vectors for Ra=10^2.

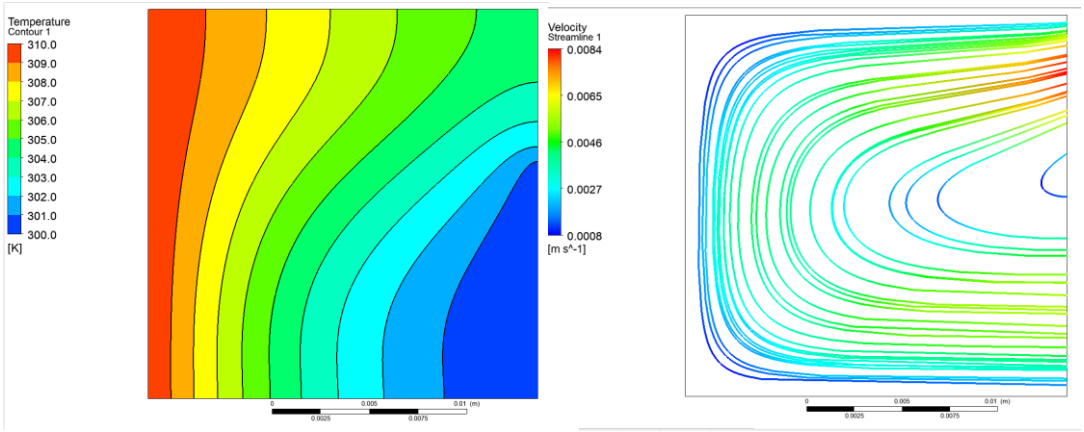

a) b)

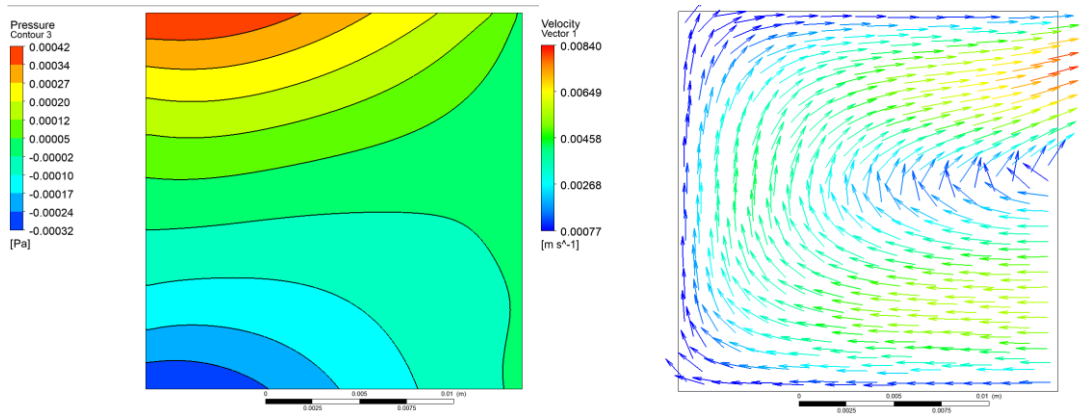

c) d)

Figure 4. 9 : a) Isotherms, b) Streamlines, c) Pressure contours, d) Velocity vectors for Ra=10^3.

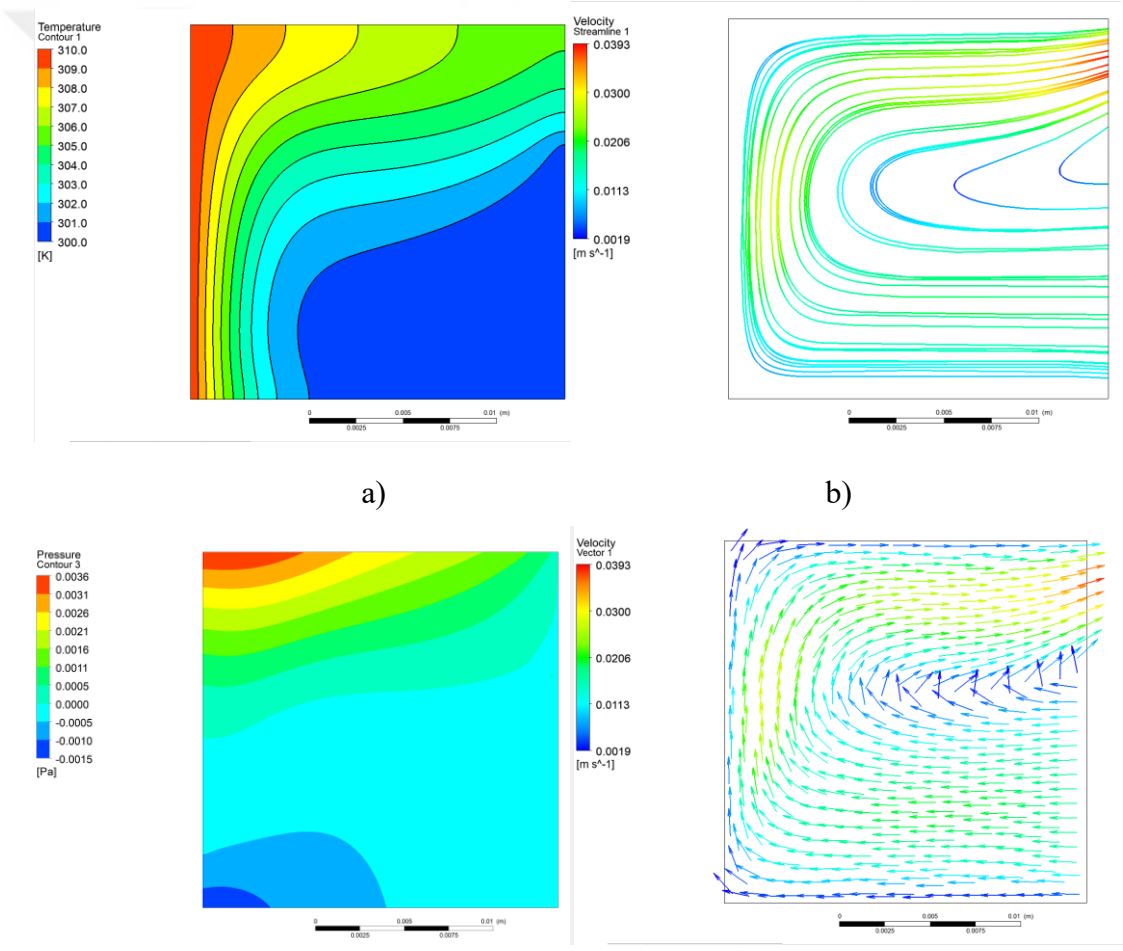

a) b)

c) d)

Figure 4. 10 : a) Isotherms, b) Streamline, c) Pressure contours, d) Velocity vectors for Ra=10^4.

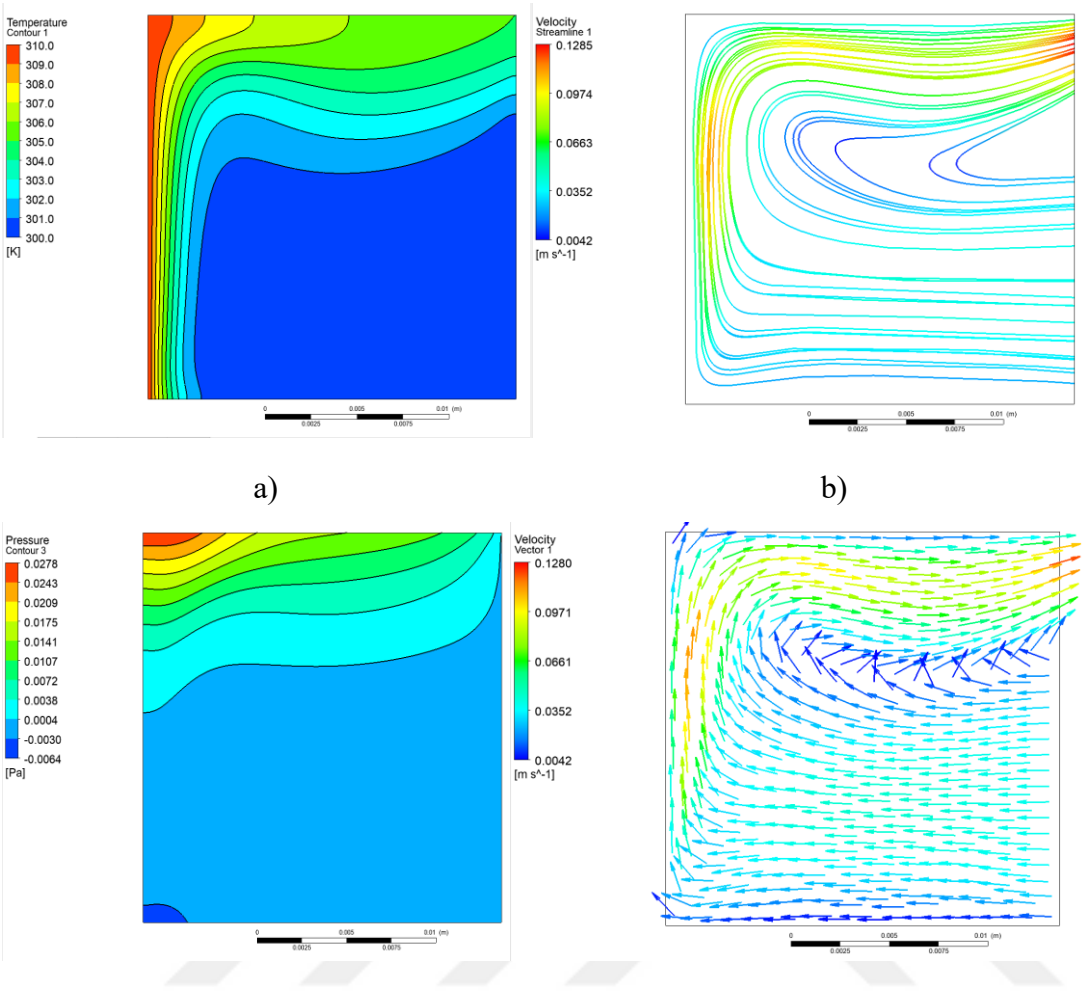

Figure 4. 11 : a) Isotherms, b) Streamlines, c) Pressure contours, d) Velocity vectors for Ra=10^5.

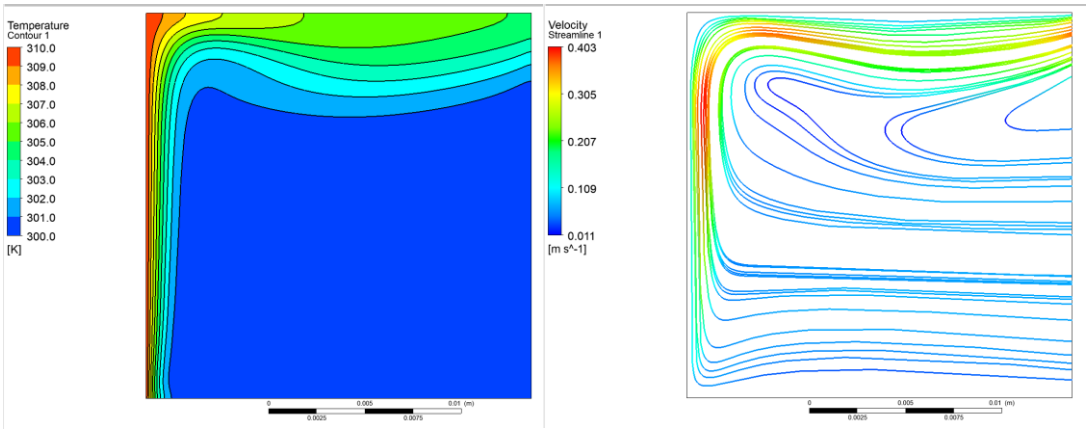

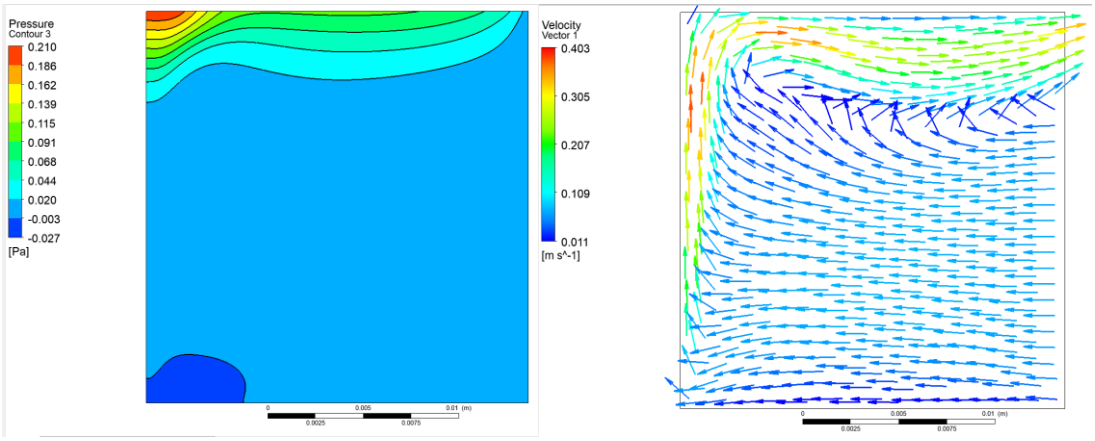

c) d)

Figure 4. 12 : a) Isotherms, b) Streamlines, c) Pressure contour, d) Velocity vectors for Ra=10^6.

Table 4. 4 : Nusselt number results for pure natural convection in a solar square cavity receiver made from aluminum.

Operating conditions		Heat flux	Average Nusselt numbers for hot wall					
Ra	Gravity, m/s^2	Total heat flux on the hot wall, W/m^2	**present study (Pr=0,71)**	Hinojosa et al.[6] (Pr= 0,71)	Bilgen and Oztop[5] (Pr= 0,72)	Shirvan et al.[17]	Chan and Tien. (Pr=1)	Karakaya and Durmuş[3] (Pr= 0,71)
10^2	0,13	11,57	**0,887**					
10^3	1,3	16,22	**1,242**	1,300	1,310	1,210	1,070	1,330
10^4	13	44,71	**3,425**	3,440	3,530	3,480	3,410	3,540
10^5	130	97,94	**7,503**	7,440	7,850	7,780	7,690	7,680
10^6	1300	191,21	**14,648**	14,510	15,200	15,150	15,000	19,350

Table 4. 5 : Nusselt number results for pure natural convection of solar square cavity receiver in which hot wall made from copper and insulated walls are made from wood.

Operating conditions		Heat flux	Average Nusselt numbers for hot wall					
Ra	Gravity, m/s^2	Total heat flux on the hot wall, W/m^2	**present study (Pr=0,71)**	Hinojosa et al.[6] (Pr= 0,71)	Bilgen and Oztop[5] (Pr= 0,72)	Shirvan et al.[17]	Chan and Tien. (Pr=1)	Karakaya and Durmuş[3] (Pr= 0,71)
10^2	0,13	11,57	**0,887**					
10^3	1,3	16,22	**1,242**	1,300	1,310	1,210	1,070	1,330
10^4	13	44,71	**3,425**	3,440	3,530	3,480	3,410	3,540
10^5	130	97,94	**7,503**	7,440	7,850	7,780	7,690	7,680
10^6	1300	191,21	**14,648**	14,510	15,200	15,150	15,000	19,350

4.2.3 Pure natural convection analysis in a fully open tilted square cavity

Problem definition: The schematic of the fully open tilted square cavity is given in Figure 2.4. There is an open square cavity with H=1 m, heated from left sidewall with temperature of 350 K and cooled by opening wall with an ambient temperature of 300 K and bottom and top walls are adiabatic. The pure natural convection for a 2D, laminar, incompressible and steady state flow was investigated. The Boussinesq approximation was applied for the density of the fluid. The Rayleigh numbers from 10^3 to 10^6 was taken as the changing parameter of the validation study.

In order to validate this study, the calculated Nusselt number, was compared with both Hinojosa and Mohamad's published results. As can be seen from Table 4.6 the Nusselt numbers results are more close to the published ones. In order to understand clearly the tilt angle effect on the heat loss in a fully open square cavity, the isotherms and velocity vectors for different tilt angles for Ra= 10^6 are given in Figure 4.13 and Figure 4.14. As can be seen from Figure 4.13. at which temperature for different tilt angles are given, the minimum natural convection **heat loss** for all Rayleigh numbers occurs when **φ** = 180°, at which solar cavity receiver opening face direction is downward. On the other hand, the maximum heat loss occurs when **φ** = 60° for the Rayleigh number of 10^3 and 10^4, and when **φ** = 75° for the Rayleigh number of 10^5 and 10^6. As tilt angle increases up to **φ** = 60 ° for Ra= 10^3 and 10^4 and up to **φ** = 75° for Ra= 10^5 and 10^6, the heat loss increases slightly and then after that angles the heat loss decreases as dramatically.

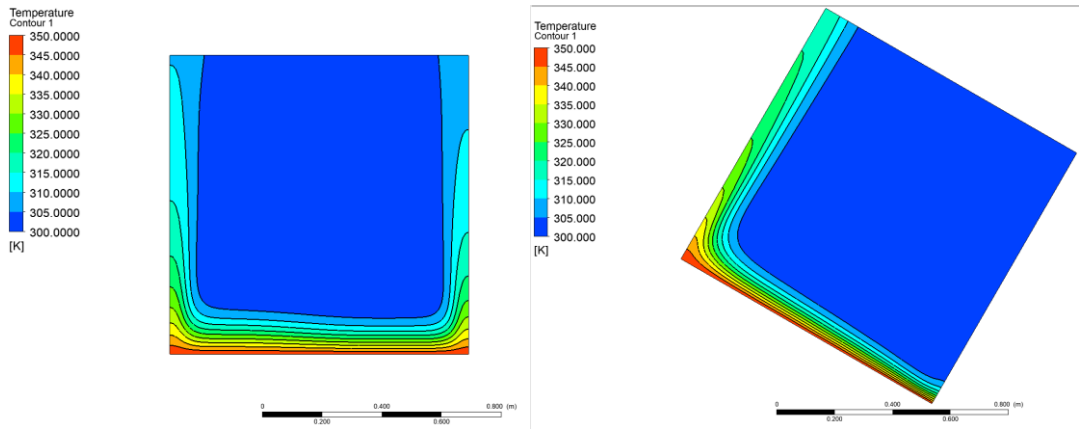

a) φ = 0° b) φ = 30°

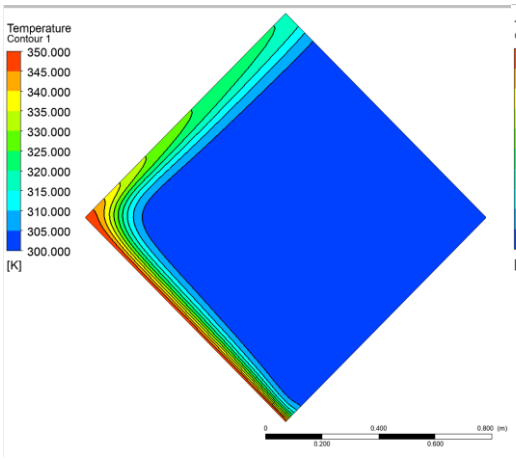

c) φ = 45°

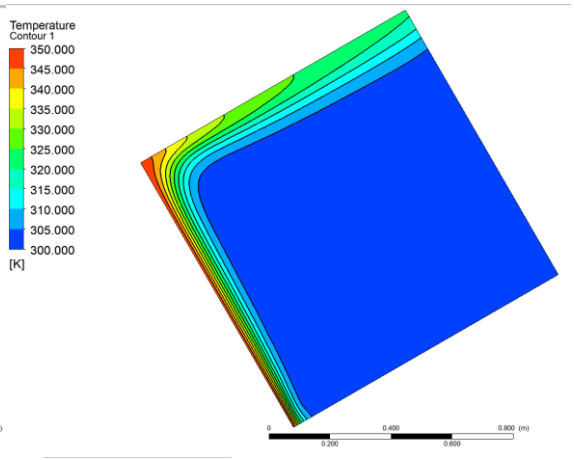

d) φ = 60°

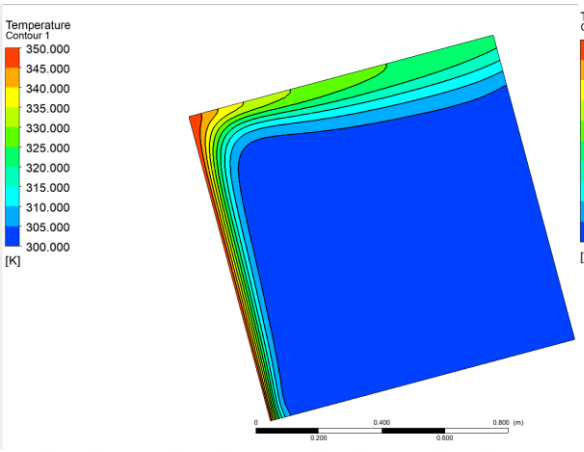

e) φ = 75°

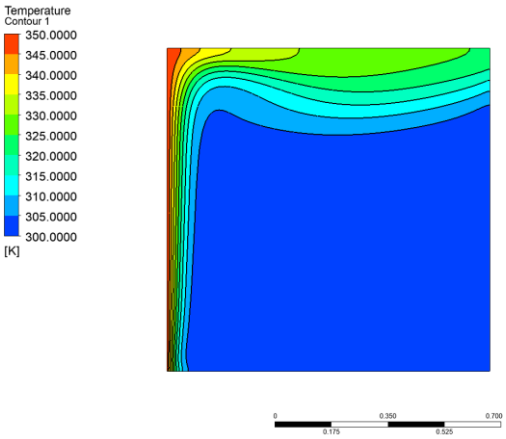

f) φ = 90°

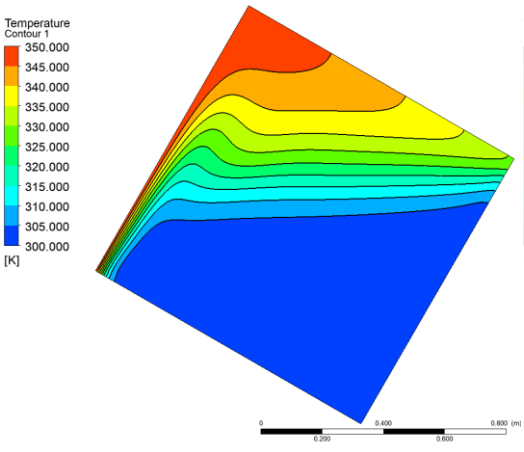

g) φ = 120°

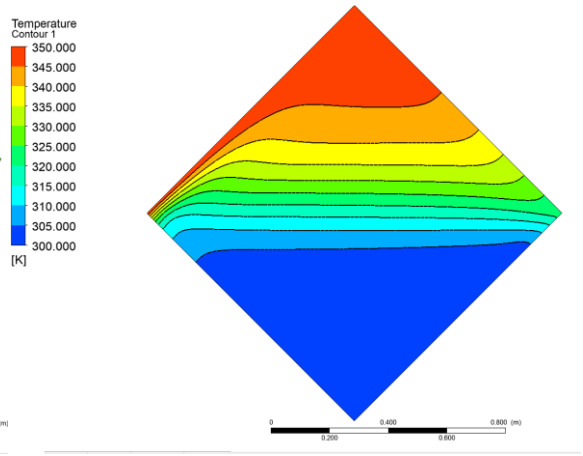

h) φ = 135°

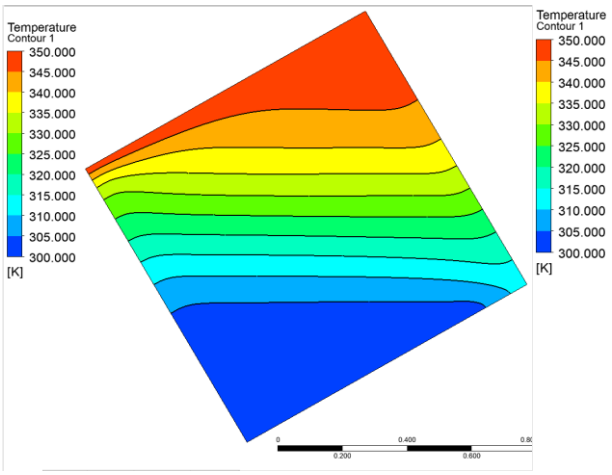

i) φ = 150°

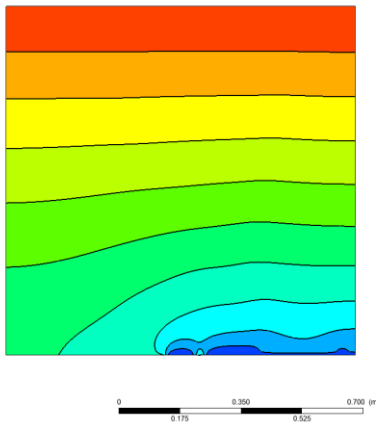

j) φ = 180°

Figure 4. 13 : Isotherms for different tilt angles for an fully open square cavity for Ra= 10^6.

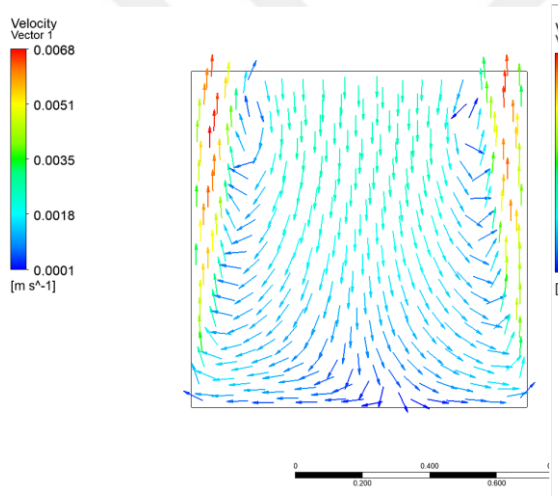

a) φ = 0°

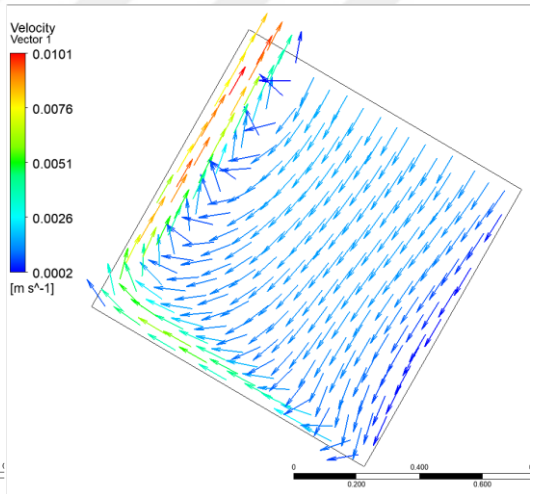

b) φ = 30°

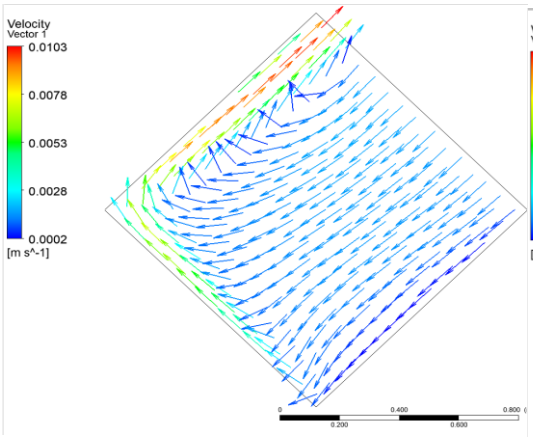

c) φ = 45°

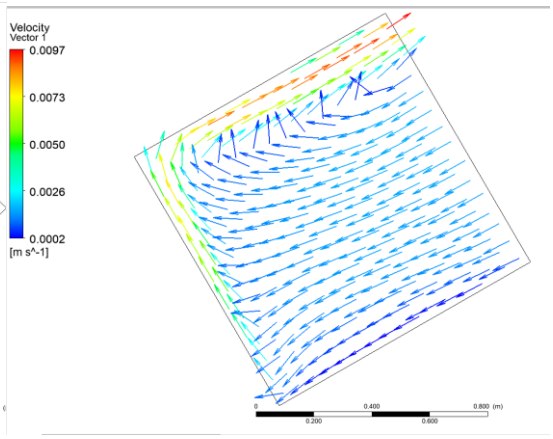

d) φ = 60°

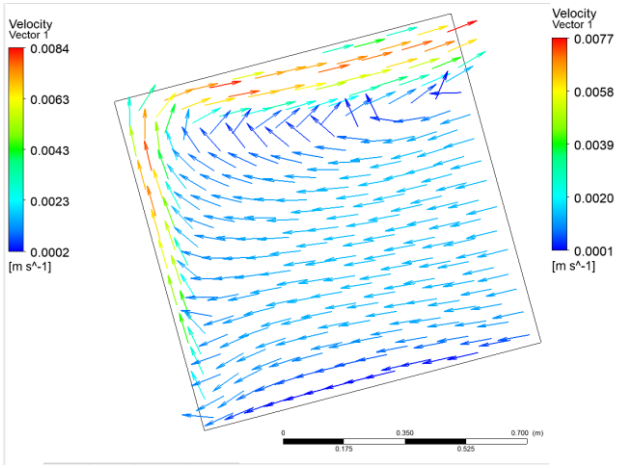

e) φ = 75°

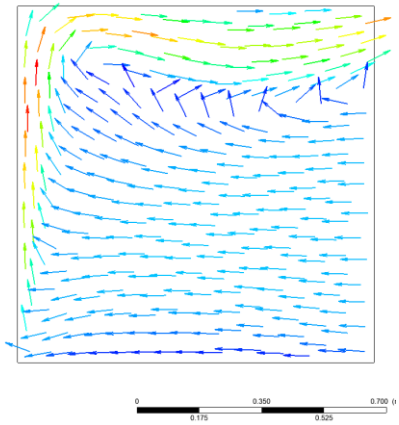

f) φ = 90°

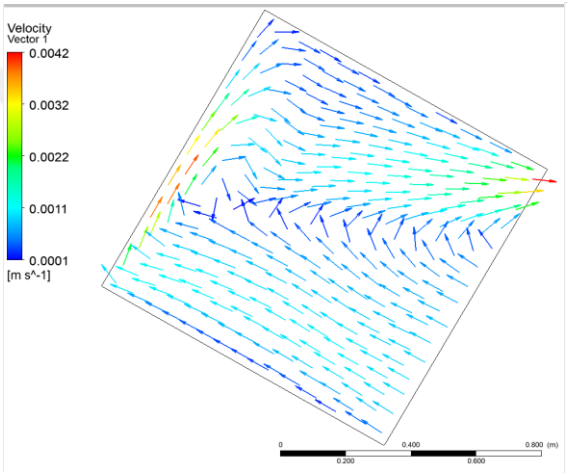

g) φ = 120°

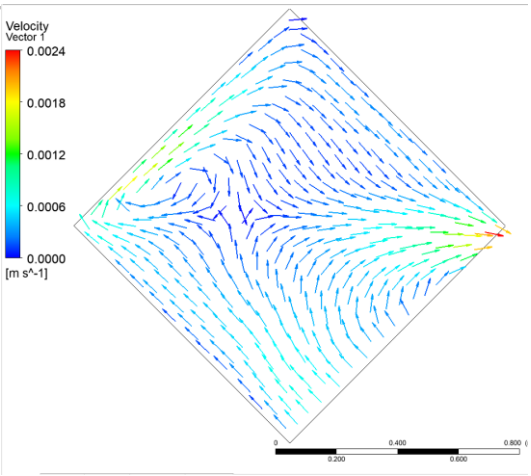

h) φ = 135°

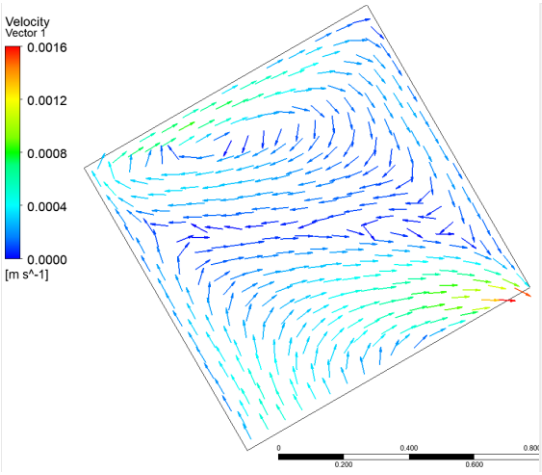

i) φ = 150°

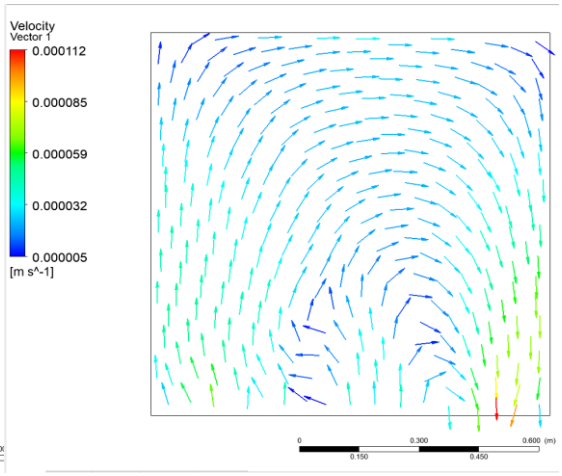

j) φ = 180°

Figure 4. 14 : Velocity vectors for different tilt angles for an fully open square cavity for Ra= 10^6.

Table 4. 6 : Pure natural convection thermal analysis results for an inclined solar square cavity receiver.

Pure natural convection in an inclined open square cavity						
Operating conditions			Heat flux	Average Nusselt numbers for hot wall		
Ra	inclination angle, degree	Gravity, m/s^2	Total heat flux on the hot wall, W/m^2	present study	Mohamad (1995) [6]	Hinojosa et al.(2005 & 2012) [6]
10^3	0	2,1E-06	**1,23**	**0,94**		
	30		1,63	1,25		
	45		1,72	1,32		
	60		1,75	1,34		
	75		1,71	1,31		
	90		1,63	1,25		
	120		1,41	1,08		
	135		1,29	0,99		
	150		1,19	0,91		
	180		1,03	0,79		
10^4	0	0,000021	**3,34**	**2,56**		2,47
	30		4,51	3,45	3,34	3,34
	45		4,79	3,67		3,59
	60		4,92	3,77	3,7	3,69
	75		4,84	3,71		
	90		4,49	3,44	3,44	3,44
	120		2,94	2,26		2,3
	135		2,08	1,59		1,63
	150		1,5	1,15		1,15
	180		1,03	0,79		1
10^5	0	0,00021	9,78	7,50		
	30		8,51	6,52	6,17	6,42
	45		9,32	7,14		
	60		9,78	7,49	7,36	7,4
	75		9,98	7,64		
	90		9,82	7,53	7,41	7,44
	120		6,27	4,80		
	135		3,43	2,63		
	150		1,9	1,46		
	180		0,96	0,73		
10^6	0	0,0021	11,07	8,48		8,79
	30		16,46	12,61	12,08	12,25
	45		17,89	13,70		13,41
	60		18,74	14,36	13,72	14,15
	75		19,19	14,70		
	90		19,17	14,69	14,36	14,51
	120		12,33	9,45		9,37
	135		5,27	4,04		4,03
	150		2,27	1,74		1,75
	180		1,02	0,78		1

4.2.4 Pure natural convection analysis in a partially open square cavity for φ= 90^{o}

Problem definition: The schematic of a partially open square cavity is given in Figure 2.5. There is an open square cavity heated from left sidewall with temperature of 310 K and cooled by opening wall with temperature of 300 K and bottom and top walls are adiabatic. The pure natural convection for a laminar, incompressible steady state flow was investigated.

The cavity is partially open such as AR = h/H = 0.50, AP = d/H = 0.50, φ= 90^{o}.

As can be seen from the Table 4.7, in which a comparison of the Nusselt numbers between a fully open square cavity and a partially open square cavity was shown, as the cavity aperture size increases the Nusselt number increases which means that natural convection heat loss increases. Therefore, in order to reduce the heat losses due to pure natural convection, cavity aperture size can be reduced in other words a partially open square cavity can be used.

The validation was done by comparing the present solution results with Bilgen Öztop results. As can be seen from Figure 4.15 to Figure 4.23, isotherms and streamlines are similar to the Bilgen and Öztop's results.

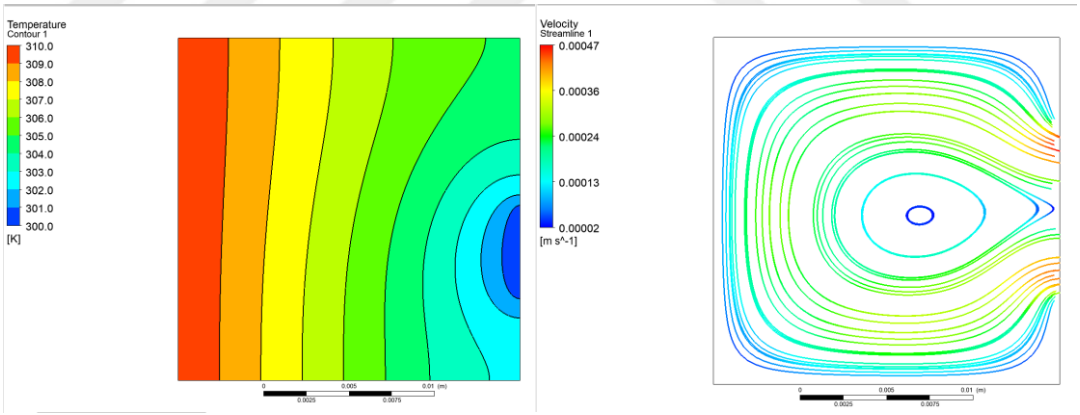

Figure 4. 15 : Isotherms and streamline results from left to right respectively for Ra= 10^{2}.

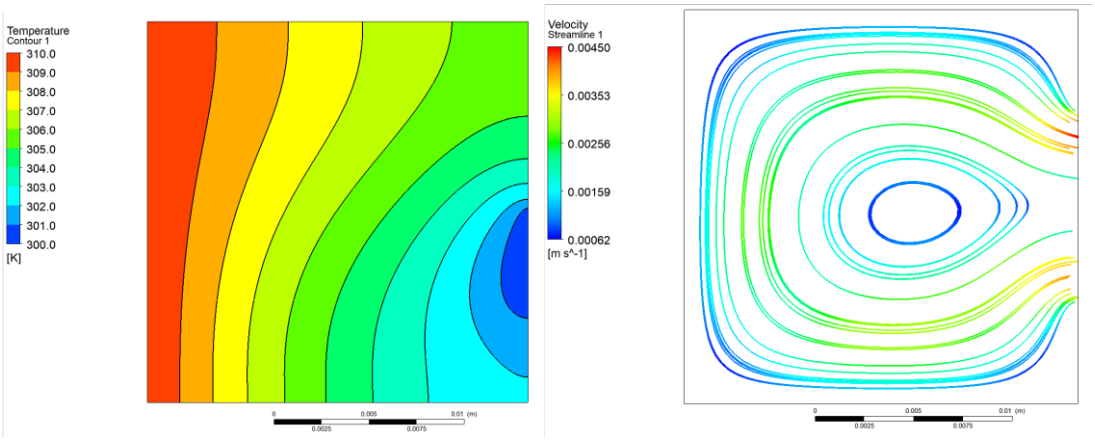

Figure 4. 16 : Isotherms and streamline results from left to right respectively for Ra= 10^3.

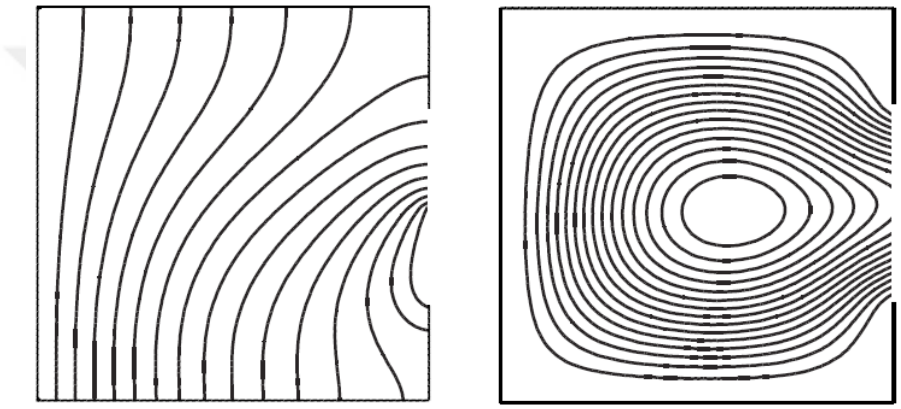

Figure 4. 17 : Isotherms and streamline results from left to right respectively for Ra= 10^3 Bilgen and Öztop results [2].

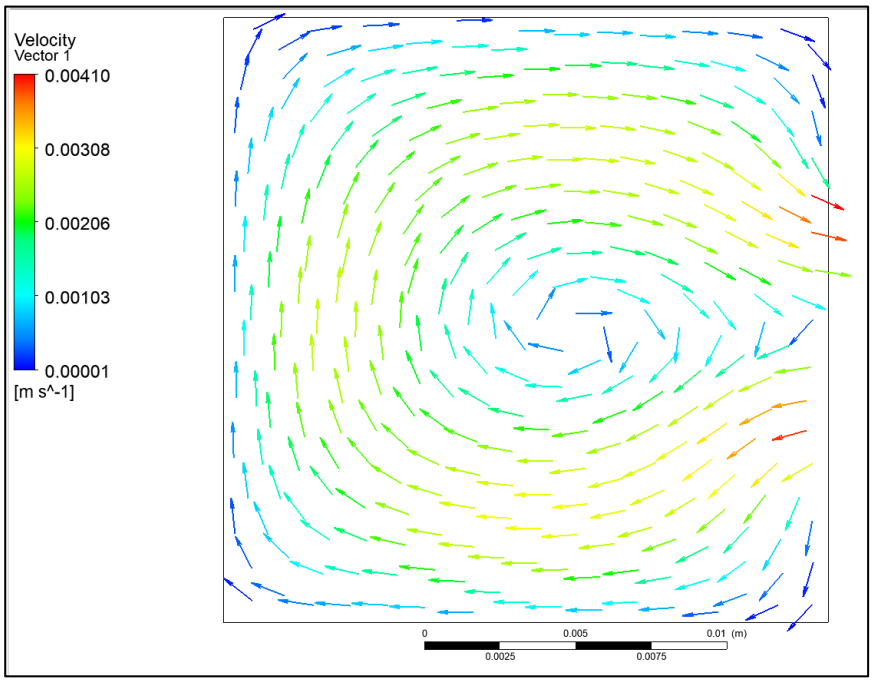

Figure 4. 18 : Velocity vector for Ra=10^3.

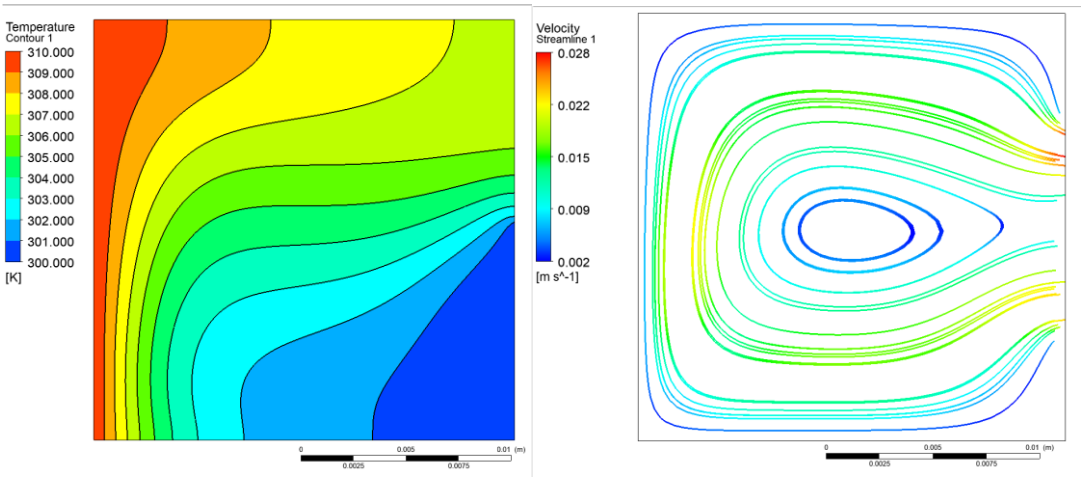

Figure 4. 19 : Isotherms and streamline results from left to right respectively for Ra= 10^4.

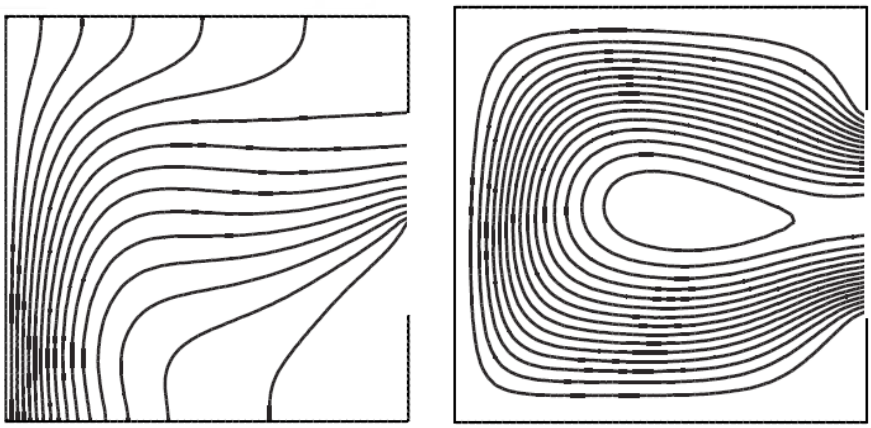

Figure 4. 20 : Isotherms and streamline results from left to right respectively for Ra= 10^4 Bilgen and Öztop results [2].

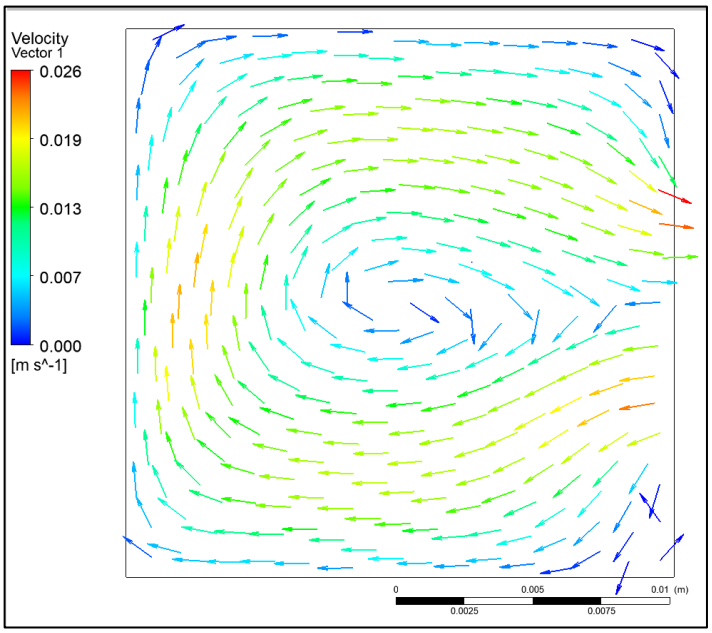

Figure 4. 21 : Velocity vector for Ra=10^4.

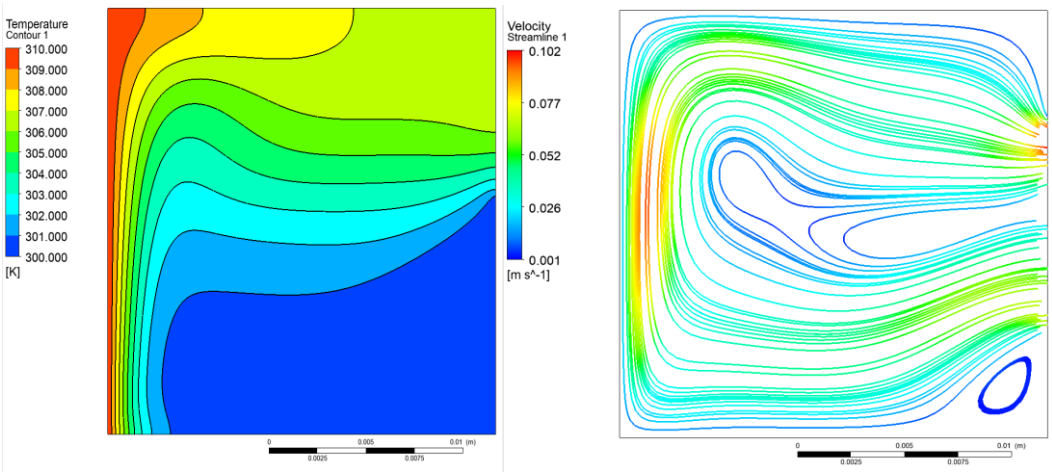

Figure 4. 22 : Isotherms and streamline results from left to right respectively for Ra= 10^5.

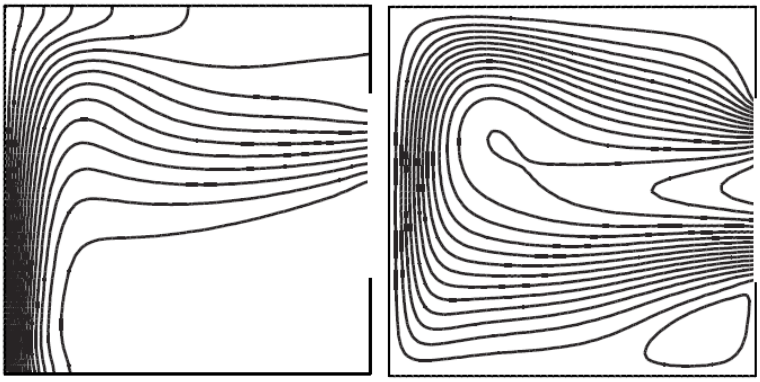

Figure 4. 23 : Isotherms and streamline results from left to right respectively for Ra= 10^5 Bilgen and Öztop results [2].

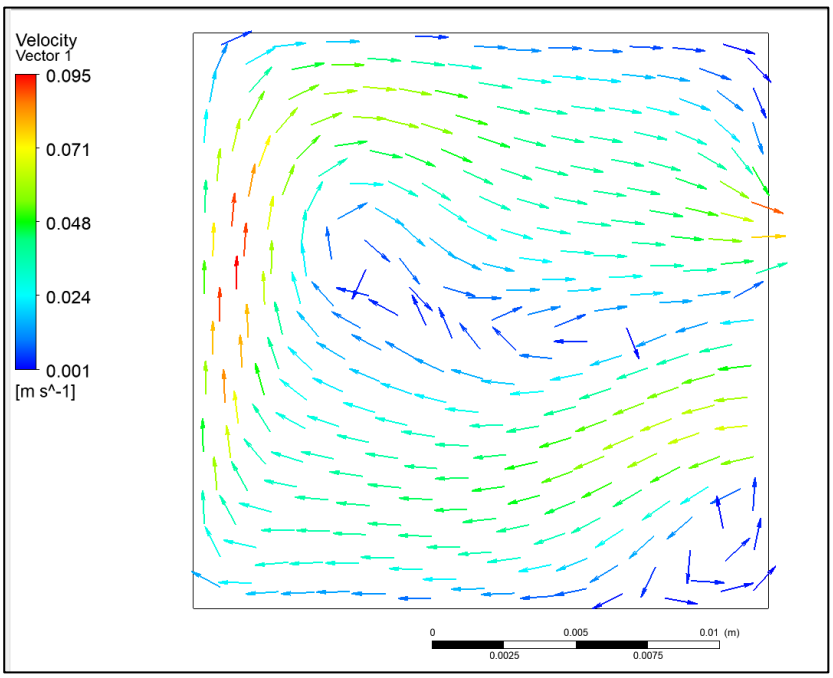

Figure 4. 24 : Velocity vector for Ra=10^5.

Table 4. 7 : Nusselt numbers comparison for a fully and partially open square cavity.

	Average Nusselt number comparison for the hot wall	
Ra	Fully open square cavity	Partially open square cavity
$\mathbf{10^2}$	0,887	0,756
$\mathbf{10^3}$	1,242	0,870
$\mathbf{10^4}$	3,425	2,518
$\mathbf{10^5}$	7,503	6,629
$\mathbf{10^6}$	14,648	13,723

4.2.5 Combined pure natural convection and surface radiation thermal analysis for a fully open square cavity

There was carried out a few validation studies. The first validation study was the surface thermal radiative model comparison with the Hinojasa et al. In order to do this, the natural convection was suppressed and the temperature of the vertical heated wall of the cavity fixed at 310 K, while the two horizontal walls and the aperture were maintained to a constant temperature of 300 K. The cavity walls and its opening are assumed as gray bodies **(ε=1)**. The fluid was considered to be radiatively nonparticipating. The comparison between the dimensional surface radiative fluxes of this study and the Hinojosa et al. [22] was presented in Table 4.8. The maximum percentage difference was 0,3 %. The tilt angle in this case is $\varphi = 90^o$.

Table 4. 8 : Validation results of surface thermal radiative model (S2S).

	Area-Weighted average radiation heat flux, W/m^2		
Wall	Present study	Hinojosa et al.[22]	Difference, %
Hot	64,362	64,365	-0,005%
Top horizontal	-18,809	-18,853	-0,233%
Bottom horizontal	-18,809	-18,853	-0,233%
Aperture	-26,742	-26,661	0,304%

The second validation study was the Nusselt number comparison for different Rayleigh numbers with the published ones. The hot wall temperature was taken as 310 K, two-horizontal walls were adiabatic, and the opening wall boundary condition was taken as Pressure Inlet with a constant temperature of 300 K. So the $\Delta T = 10$ K was taken for this validation. The fluid was assumed to be air (Pr= 0,71) and Newtonian and fluid flow was considered to be laminar. The fluid properties were taken as constant except for the density in the buoyancy force, the Boussinesq

approximation was applied. The cavity walls and its opening assumed as blackbody and emissivity of all walls were taken as **ε=1** and the fluid is nonparticipating to the radiation. The Table 4.9 shows the convective, radiative and total average Nusselt numbers comparison with published ones for different Rayleigh numbers.

The tilt angle in this case was also equal to 90^{o}.

The Rayleigh number changed by open square cavity dimensions and the gravity was kept constant (9,81 m/s^2) in this case. The comparison of Nusselt numbers indicates that, the calculated Nusselt numbers are more close to the published results. As seen from Table 4.9 as Rayleigh number increases, the heat loss increases, and radiation heat loss becomes dominant at high Rayleigh numbers. The results show that mathematical model and Ansys Fluent Thermal Analysis results were validated.

Table 4. 9 : Average Nusselt number (for hot wall) comparison with published ones.

Average Nusselt Number Results Comparision														
Operating condition for present study		Present study						Hinojosa and Estrada [22]				Shirvan et al [17]		
Ra	H, mm present study dimensions	Total Surface Heat Flux, W/m^2	Radiation Heat Flux, W/m^2	Nr	**Nu(Conv)**	**Nu(Rad)**	**Nu(Total)**	Nr	Nu(Conv)	Nu(Rad)	Nu(Total)	Nu(Conv)	Nu(Rad)	Nu(Total)
10^2	4,73	89,75	36,53	8,89	**0,96**	**0,66**	**1,63**							
10^3	10,2	70,77	37,89	19,17	**1,28**	**1,48**	**2,77**	20,54	1,19	1,73	2,92	1,35	1,80	3,15
10^4	21,97	77,65	40,94	41,29	**3,09**	**3,44**	**6,53**	44,26	2,98	3,72	6,70	3,15	4,01	7,16
10^5	47,34	79,33	43,05	88,97	**6,58**	**7,81**	**14,39**	95,35	6,40	8,02	14,42	6,50	8,08	14,58
10^6	101,99	76,97	44,27	191,68	**12,78**	**17,29**	**30,07**	205,40	12,43	17,29	29,72	12,58	17,38	29,96

4.3 Thermal Analysis of a Solar Cavity Receiver

For solar cavity receiver, the hot wall material is made from copper and the insulated wall material is made from wood, so emissivity of those materials were found and the validated mixed thermal analysis problem in part 4.2.6 was repeated, and the results were given in Table 4.10. The Rayleigh numbers changed by solar cavity receiver dimension and the gravity was kept constant (9,81 m/s^2) in this case. The temperature difference was 10 K. As can be seen from the Table 4.10 for a solar cavity receiver the main heat loss at low temperature differences occurs due to natural convection. When the Nusselt numbers Results found in this case was compared with the Nusselt numbers found in Table 4.9, **the emissivity effect** could be understood easily that, as emissivity of material of the cavity wall increases, the

heat loss increases due to radiation and therefore total heat loss increases. Furthermore, as increasing the dimension of the open square cavity, Rayleigh number increases so that heat loss increases.

Table 4. 10 : Thermal analysis of a solar square cavity receiver for ΔT= 10 K.

Average Nusselt number results comparison for hot wall										
Operating condition for present Study					**Present study**					
Ra	ε, copper, hot wall	ε, wood, insulation	H, mm present study dimensions	g, m/s^2	Total surface heat flux, W/m^2	Radiation heat flux, W/m^2	Nr	**Nu(Conv)**	**Nu(Rad)**	**Nu(Total)**
$\mathbf{10^2}$	0,1	0,95	4,73	9,81	67,45	3,91	8,89	**1,15**	**0,07**	**1,22**
$\mathbf{10^3}$	0,1	0,95	10,2	9,81	45,86	4,20	19,17	**1,63**	**0,16**	**1,79**
$\mathbf{10^4}$	0,1	0,95	21,97	9,81	48,19	4,63	41,29	**3,67**	**0,39**	**4,06**
$\mathbf{10^5}$	0,1	0,95	47,34	9,81	46,67	4,98	88,97	**7,56**	**0,90**	**8,46**
$\mathbf{10^6}$	0,1	0,95	101,99	9,81	42,21	5,24	191,68	**14,44**	**2,05**	**16,49**

In order to investigate the reasons of heat losses in detail for a solar cavity receiver, temperature difference effect, dimension changing effect and effect of tilt angle of solar cavity were studied respectively for a solar cavity receiver.

4.3.1 Temperature difference effect on the heat loss mechanism of solar cavity receiver for Ra= 10^6

The other case studied was the temperature difference effect on the heat loss in a solar cavity receiver. In order to do this, a 1 m length 2D square solar cavity receiver was modeled since the total heat loss in large dimension change was found high at the previous studies. The temperature difference effect was investigated just for Ra= 10^6. The air temperature coming from opening was kept constant as 300 K, but hot wall temperature was increased to investigate its effect on the heat loss.

The temperature difference effect on the heat loss was studied and the results are in the Table 4.11, indicate that as the temperature difference increases, the heat loss increases mostly due to radiation effect. The Nusselt number for radiation increases dramatically while it almost remains same for natural convection as hot wall temperature increases.

The tilt angle in this case is φ= 90^o.

Table 4. 11 : The temperature difference effect on the heat loss, and Nusselt number, for Ra=10^6.

Average Nusselt number results comparison for hot wall for different temperature difference for Ra= 10^6									
ΔT	g	ε, copper, hot wall	ε, wood, insulation	H, mm present study dimensions	Total surface heat flux, W/m^2	Radiation heat flux, W/m^2	**Nu(Conv)**	**Nu(Rad)**	**Nu(Total)**
10	0,0104	0,1	0,95	1000	9,96	5,77	16,0	22,1	38,1
50	0,00208	0,1	0,95	1000	56,33	35,46	16,0	27,2	43,2
100	0,00104	0,1	0,95	1000	132,3	90,77	15,7	34,3	50,0
150	0,000693	0,1	0,95	1000	233,95	172,02	15,8	43,9	59,7
200	0,00052	0,1	0,95	1000	368,14	286	15,7	54,8	70,5

4.3.2 The dimension effect on the heat loss in solar cavity receiver for Ra= 10^6

In this case, different dimensions of solar square cavity receiver were studied to investigate its effect on the heat loss. The air temperature coming from opening was kept constant as 300 K and hot wall temperature was kept constant as 310 K. Then, different dimensions of solar cavity receiver were investigated for Ra=10^6. The results in Table 4.12 shows that as length of solar square cavity increases, there is a dramatic increase in the radiation heat loss and on the other hand, there is a slightly increase in the convection heat loss. As the length of solar square cavity increases, the convection heat loss percentage decreases from 97% to 42 %, which means that, radiation heat loss becomes dominant. The tilt angle in this case is φ= 90^o.

Table 4. 12 : Average Nusselt number results for different dimensions of solar square cavity receiver for Ra= 10^6.

		Heat flux for hot wall			**Average Nusselt numbers for hot wall**				
H= L, mm	g, m/s^2	Total surface heat flux, W/m^2	Radiation heat flux, W/m^2	Convection heat flux, W/m^2	**Nu(Conv)**	**Nu(Rad)**	**Nu(Total)**	**% of convection**	**% of radiation**
20	1300	191,2	5,01	186,19	14,27	0,38	14,65	97%	3%
100	10,41	42,92	5,24	37,68	14,43	2,01	16,44	88%	12%
200	1,3	24,79	5,42	19,37	14,83	4,15	18,98	78%	22%
500	0,083	13,76	5,64	8,12	15,55	10,80	26,35	59%	41%
1000	0,0104	9,96	5,77	4,19	16,04	22,10	38,14	42%	58%

4.3.3 Combined natural convection and surface radiation analysis results for a tilted solar square cavity receiver

In this case the copper material emissivity = 0,1 and wood material emissivity= 0,95. Since, the focus of this study is investigation of thermal solar cavity receiver, the selected temperature properties were: T_C = 300 K, T_H = 350 K, ΔT = 50 K, and H= 1 m. As seen from Table 4.13, the maximum heat loss occurs due to radiation. The maximum heat loss in this case occurs when tilt angle is 180^o for Rayleigh numbers 10^3 and 10^4. On the other hand, for Rayleigh numbers of 10^5 and 10^6, the maximum heat losses occur at tilt angles of 75^o and 90^o respectively. The convection Nusselt number changes with tilt angle substantially except for $\varphi = 180^o$ there was a little increase in $Ra=10^6$. The radiation Nusselt number does not change substantially with tilt angle because the dimension of the cavity was kept constant and just gravity was changed so there was no effect of tilt angle on the radiation heat loss.

In addition, as Rayleigh number increases, the maximum heat loss increases at different angles of tilt. In addition, as seen from Table 4.13, the minimum heat loss occurs at $\varphi = 45^o$ for $Ra=10^3$, $\varphi = 0^o$ for $Ra= 10^4$, and $\varphi = 180^o$ for $Ra= 10^5$ and 10^6.

In brief, there is a nonlinear relationship with heat loss and tilt angle.

Table 4. 13 : Tilt angle effect on combined heat loss in solar cavity receiver for different Rayleigh numbers.

Combined natural convection and surface radiation in an inclined open square cavity								
Operating conditions			Heat flux for hot wall, W/m^2			Average Nusselt numbers for hot wall		
Ra	inclination angle, degree	Gravity, m/s^2	Total heat flux	Radiation heat flux	Convection heat flux	N(tot)	Nu(rad)	Nu(conv)
10^3	0	2E-06	42,89	35,8	7,09	32,86	27,43	5,43
	30		41,79	34,86	6,93	32,02	26,71	5,31
	45		41,75	34,798	6,952	**31,99**	26,66	5,33
	60		41,76	34,79	6,97	31,99	26,65	5,34
	75		41,88	34,88	7	32,08	26,72	5,36
	90		41,9	34,91	6,99	32,09	26,74	5,35
	120		41,86	34,91	6,95	32,07	26,75	5,32
	135		41,91	34,96	6,95	32,11	26,79	5,32
	150		41,97	35,02	6,95	32,15	26,83	5,32
	180		43,64	36,39	7,25	**33,43**	27,88	**5,55**
10^4	0	2E-05	40,91	33,64	7,27	**31,34**	25,77	5,57
	30		43,06	34,63	8,43	32,99	26,53	6,46
	45		43,31	34,59	8,72	33,18	26,50	6,68
	60		43,24	34,61	8,63	33,12	26,51	6,61
	75		43,23	34,54	8,69	33,12	26,46	6,66
	90		43,15	34,61	8,54	33,05	26,51	6,54
	120		42,77	34,87	7,9	32,76	26,71	6,05
	135		42,59	35,03	7,56	32,63	26,84	5,79
	150		42,45	35,18	7,27	32,52	26,95	5,57
	180		43,89	36,54	7,35	**33,62**	27,99	**5,63**
10^5	0	0,0002	47,27	35,28	11,99	36,21	27,03	9,18
	30		46,8	35,66	11,14	35,85	27,32	8,53
	45		47,48	35,53	11,95	36,37	27,22	9,15
	60		47,85	35,39	12,46	36,65	27,11	9,54
	75		47,96	35,23	12,73	**36,74**	26,99	9,75
	90		47,77	35,03	12,74	36,6	26,84	9,76
	120		46,15	35,11	11,04	35,36	26,90	8,46
	135		45	35,39	9,61	34,48	27,12	7,36
	150		44,17	35,66	8,51	33,84	27,32	6,52
	180		43,46	35,81	7,65	**33,3**	27,44	**5,86**
10^6	0	0,0021	50,68	35,75	14,93	38,83	27,39	11,44
	30		52,09	36	16,09	39,91	27,58	12,33
	45		54,3	35,89	18,41	41,6	27,50	14,10
	60		55,45	35,77	19,68	42,48	27,40	15,08
	75		56,25	35,66	20,59	43,09	27,32	15,77
	90		56,38	35,46	20,92	**43,2**	27,17	16,03
	120		53,03	35,37	17,66	40,63	27,10	13,53
	135		49,45	35,59	13,86	37,88	27,26	10,62
	150		46,82	35,77	11,05	35,87	27,40	8,47
	180		44,44	35,9	8,54	**34,05**	27,51	**6,54**

5. CONCLUSIONS AND RECOMMENDATIONS

In this thesis study, for a 2D open square cavity, laminar, steady state flow was studied for respectively pure natural convection heat transfer and combined natural convection and surface radiation heat transfer. Different factors acting on the heat loss in an open square cavity were investigated and the results were validated by comparing with the published results. At the beginning of the study, a closed square cavity was studied to understand the pure natural convection heat transfer phenomena and to set up a correct mathematical model for an open square cavity. Then respectively, for validation with published literature results, a fully open square cavity, a fully open tilted square cavity, and a partially open square cavity were investigated. The most important validation keys of the study were to compare the calculated Nusselt numbers with published ones. In addition, isotherms, and streamline, velocity vector and pressure contour results were validated as Nusselt numbers were validated well with the published ones.

The lessons to be learned from the validation analysis results are those:

- The fluid inside a closed square cavity rotates clockwise due to buoyancy effect and as Rayleigh number increases, the fluid accelerates and a thermal boundary layer forms both on the hot wall and cold wall. In addition, as Rayleigh number increases, thermal boundary layer and velocity boundary layer thicknesses on the walls decreases.
- In the open square cavity, fluid enters from bottom of the cavity and reaches to the hot wall; it gets warmer there then exits from near the top wall by the buoyancy effect. A thermal boundary layer forms on the hot wall of the cavity. As Rayleigh number increases thermal boundary layer thickness and velocity boundary layer thickness on the hot wall decreases.
- There is no effect of the materials of the cavity wall on the 2D pure natural convection thermal analysis of the cavity; all the results have the same Nusselt numbers due to dominant feature of the convection on conduction.

- The results of the pure natural convection thermal analysis for an open square cavity indicates that; for a tilted cavity, the minimum natural convection heat loss for all Rayleigh numbers occurs when $\varphi = 180^{o}$, at which solar cavity receiver opening face direction is downward. On the other hand, the maximum heat loss occurs when $\varphi = 60^{o}$ for the Rayleigh number of 10^{3} and 10^{4}, and when $\varphi = 75^{o}$ for the Rayleigh number of 10^{5} and 10^{6}. As tilt angle increases up to $\varphi = 60^{o}$ for Ra= 10^{3} and 10^{4} and up to $\varphi = 75^{o}$ for Ra= 10^{5} and 10^{6}, the heat loss increases slightly and then after that angles the heat loss decreases as dramatically.
- As the cavity aperture size increases the Nusselt number increases which means that natural convection heat loss increases. Therefore, in order to reduce the heat losses due to pure natural convection, cavity aperture size can be reduced in other words a partially open square cavity can be used.
- The thermal analysis results for a combination of natural convection and surface radiation indicates that as Rayleigh number increases, the heat loss increases, and radiation heat loss becomes dominant at high Rayleigh numbers.

Then, temperature difference, tilt angle factors acting on the heat loss in a 2D, square solar cavity receiver with 1 m dimension were investigated. In addition, cavity dimension changing effect on the heat loss in a solar square cavity was studied.

The lessons to be learned from this thermal analysis of a solar square cavity ($\varphi = 90^{o}$) are those:

- As emissivity increases, radiation heat loss increases so total heat loss increases in the cavity. The Nusselt number for radiation increases dramatically while it almost remains same for natural convection as hot wall temperature increases.
- As hot wall temperature of the cavity increases, the total heat loss in solar cavity receiver increases due to radiation losses.
- As dimensions of solar square cavity increases, there occurs a dramatic increase in the radiation heat loss and on the other hand, there occurs a slightly increase in the convection heat loss.
- There was found a nonlinear relationship with tilt angle and heat loss.

To sum up, in order to reduce the heat loss in a solar square cavity receiver, a partially open square cavity, with small dimension and low emissivity materials of cavity walls could be used.

REFERENCES

[1] **Elatar A., Teamah M., Hassab M.** (2015). Numerical study of laminar natural convection inside square enclosure with single horizontal fin. *International Journal of Thermal Sciences 99 (2016) 41-51.*

[2] **Bairi A.** (2008). Nusselt–Rayleigh correlations for design of industrial elements: Experimental and numerical investigation of natural convection in tilted square air filled enclosures. *Energy Conversion and Management 49 (2008) 771–782.*

[3] **Karakaya H., Durmuş A.** (2016). Numerical and experimental study of air flow by natural convection in a rectangular open cavity cooled top and bottom surfaces. *Journal of Life Sciences; Volume 6 Number 2/2.*

[4] **Kumar S.** (2009). *CFD analysis of natural convection in differentially heated enclosure* (Master's thesis). Department of Mechanical Engineering, National Institute of Technology Rourkela.

[5] **Bilgen E., Oztop H.** (2005). Natural convection heat transfer in partially open inclined square cavities. *International Journal of Heat and Mass Transfer 48 (2005) 1470–1479.*

[6] **Hinojosa J.** (2012). Numerical study of the natural convection in a two dimensional partially open tilted cavity. *Latin American Applied Research. 42:267-274.*

[7] **Bilgen E., Muftuoglu A.** (2005). Natural convection in an open square cavity with slots. *International Communications in Heat and Mass Transfer 35 (2008) 896–900.*

[8] **Prakash M., Kedare S., Nayak J.** (2012). Numerical study of natural convection loss from open cavities. *International Journal of Thermal Sciences 51 (2012) 23-30.*

[9] **Prakash M.** (2013). Numerical studies on natural convection heat losses from open cubical cavities. *Hindawi Publishing Corporation Journal of Engineering Volume 2013, Article ID 320647, 9 pages http://dx.doi.org/10.1155/2013/320647.*

[10] **Prakash M., Kedare S., Nayak J.** (2009). Investigations on heat losses from a solar cavity receiver. *Solar Energy 83 (2009) 157–17.*

[11] **Bondareva N., Sheremet M., Oztop H., Abu-Hamdeh N.** (2017). Heatline visualization of natural convection in a thick walled open cavity filled with a nanofluid. *International Journal of Heat and Mass Transfer 109 (2017) 175–186.*

[12] **Asghar M., Gorla R.** (2010). Buoyancy-driven flow of a viscous incompressible fluid in an open-ended rectangular cavity with

permeable horizontal surfaces. *International Journal of Numerical Methods for Heat & Fluid Flow Vol. 20 No. 7, 2010 pp. 759-772.*

[13] **Gonzalez M., Hinojosa J., Vidales H., Orozco A.** (2015). Theoretical and experimental study of natural convection with surface thermal radiation in a side open cavity. *Applied Thermal Engineering 75 (2015) 1176-1186.*

[14] **Gonzalez M., Palafox J., Estrada C**. (2012). Numerical study of heat transfer by natural convection and surface thermal radiation in an open cavity receiver. *Solar Energy 86 (2012) 1118–1128.*

[15] **Singh D., Singh S.** (2016). Combines free convection and surface radiation in tilted open cavity. *International Journal of Thermal Sciences 107 (2016) 111-120.*

[16] **Hinojosa J., Cabanillas R., Alvarez G., Estrada C.** (2005). Nusselt number for the natural convection and surface thermal radiation in a square tilted open cavity. *International Communications in Heat and Mass Transfer 32 (2005) 1184–1192.*

[17] **Shirvan K., Mamourian M., Mirzakhanlari S., Ellahi R., Vafai K.** (2017). Numerical investigation and sensitivity analysis of effective parameters on combined heat transfer performance in a porous solar cavity receiver by response surface methodology. *International Journal of Heat and Mass Transfer 105 (2017) 811–825*.

[18] **Hathaway B., Lipinski W., Davidson J. (2012).**Heat Transfer in a Solar Cavity Receiver: Design Considerations. *Numerical Heat Transfer, Part A:Applications, 62:5, 445-461, DOI: 10.1080/10407782.2012.703471*

[19] **Baytaş A. C.** (2015). Doğal, Zorlamalı ve Birleşik Taşınım. *Taşınım ile Isı Geçişi* (Vol.1, pp. 95-135). ANKARA: Nobel Akademik Yayıncılık Eğitim Danışmanlık Tic.Ltd. Şti.

[20] **Bellos E.and Tzivanidis C.** A review of concentrating solar thermal collectors with and without nanofluids. *Journal of Thermal Analysis and Calorimetry. Retrieved from, https://doi.org/10.1007/s10973-018-7183-1* .

[21] **Tutorial 5.** (2006). Modeling Radiation and Natural Convection *ANSYS Fluent* (pp. 38).

[22] **Hinojosa J., Estrada C., Cabanillas R., Alvarez G.** (2005). Numerical study of transient and steady-state natural convection and surface thermal radiation in a horizontal square open cavity. *Numerical Heat Transfer, Part A, 48:2, 179-196, DOI: 10.1080/10407780590948936.*

[23] **Incropera F., Dewitt D., Bergman T., Lavine A.** (2013). Radiation Exchange Between Surfaces. *Principles of Heat and Mass Transfer.* (7th ed., pp. 862-879). Singapore: John Wiley & Sons.

[24] **Halıcı F., Gündüz M. (2013).** Isı Işınımı. *Örneklerle Isı Geçişi Isı Transferi* (pp. 451- 473). Istanbul: Birsen Yayınevi.

[25] **Çengel Y.** (2012). Işınım Isı Transferi. *Isı ve Kütle Transferi.* (3rd ed. pp. 709-730).

APPENDICES

APPENDIX A: Tables

Table A. 1 : ANSYS Fluent settings for a pure natural convection in a closed square cavity.

Solution Models		
Energy	On	
Viscous	Laminar	
Fluid Properties		
Material	air	
temperature	300	K
density-Boussinesq	1,1771	kg/m^3
Cp(specific heat)	1006,3	j/kg-K
thermal conductivity	0,026107	W/m-K
Viscosity	0,000018531	kg/m-s
Kinematic viscosity	0,000015743	m^2/s
Thermal expansion coefficient	0,0033333	1/K
Thermal diffusion coefficient	0,000022039	m^2/s
Prandtl number	0,71432	
Solid Wall Material Properties		
Material of all wall	Aluminum	
Density	2719	kg/m^3
Cp(specific heat)	871	j/kg-K
thermal conductivity	202,4	W/m-K
Boundary Conditions		
Cold Wall Temperature	300	K
Cold Wall Material	Aluminum	
Hot Wall Temperature	310	K
Hot Wall Material	Aluminum	
Interior surface body material	Air	
ΔT	10	K
Insulation -Heat Flux boundary condition	0	W/m^2
Operating Conditions		
Operating Pressure	0	Pa
Gravity- Ra=E2	-0,13	m/s^2
Operating Temperature	300	K
Specified Operating Density	1,1771	kg/m^3

Solution Methods	
Pressure-Velocity Coupling	
Scheme	SIMPLE
Gradient	Least Square Cell Based
Pressure	Presto
Momentum	Second Order Upwind
Energy	Second Order Upwind
Solution Controls	
Default Values	
Residuals	
Continuity	10^{-3}
x-velocity	10^{-3}
y-velocity	10^{-3}
Energy	10^{-6}
Solution Initilization	
Standard Initialization	
Compute from	All zones

Table A. 2 : ANSYS Fluent settings for pure natural convection in an open square cavity.

Solution Models		
Energy	On	
Viscous	Laminar	
Fluid Properties		
Material	air	
temperature	300	K
density-Boussinesq	1,1771	kg/m^3
Cp(specific heat)	1006,3	j/kg-K
thermal conductivity	0,026107	W/m-K
Viscosity	0,000018531	kg/m-s
Kinematic viscosity	0,000015743	m^2/s
Thermal expansion coefficient	0,0033333	1/K
Thermal diffusion coefficient	0,000022039	m^2/s
Prandtl number	0,71432	
Solid Wall Material Properties		
Material of all wall	Aluminum	
Density	2719	kg/m^3
Cp(specific heat)	871	j/kg-K
thermal conductivity	202,4	W/m-K
Boundary Conditions		
Opening Wall Temperature	300	K
Opening Wall	Pressure inlet	
Opening Wall Pressure	0	Pa
Hot Wall Temperature	310	K
Hot Wall Material	Aluminum	
Interior surface body material	Air	
ΔT	10	K
Insulation -Heat Flux boundary condition	0	W/m^2
Operating Conditions		
Operating Pressure	0	Pa
Gravity- Ra=E2	-0,13	m/s^2
Operating Temperature	300	K
Specified Operating Density	1,1771	kg/m^3

Solution Methods	
Pressure-Velocity Coupling	
Scheme	SIMPLE
Gradient	Least Square Cell Based
Pressure	Presto
Momentum	Second Order Upwind
Energy	Second Order Upwind
Solution Controls	
Default Values	
Residuals	
Continuity	10^{-3}
x-velocity	10^{-3}
y-velocity	10^{-3}
Energy	10^{-6}
Solution Initialization	
Standard Initialization	
Compute from	All zones

Table A. 3 : ANSYS Fluent settings for combined pure natural convection and radiation thermal analysis.

Solution Models		
Energy	On	
Viscous	Laminar	
Radiation	S2S	
Fluid Properties		
Material	air	
temperature	300	K
density-Boussinesq	1,1771	kg/m^3
Cp(specific heat)	1006,3	j/kg-K
thermal conductivity	0,026107	W/m-K
Viscosity	0,000018531	kg/m-s
Kinematic viscosity	0,000015743	m^2/s
Thermal expansion coefficient	0,0033333	1/K
Thermal diffusion coefficient	0,000022039	m^2/s
Prandtl number	0,71432	
Solid Wall Material Properties		
Material of all wall	Aluminum	
Density	2719	kg/m^3
Cp(specific heat)	871	j/kg-K
thermal conductivity	202,4	W/m-K
Boundary Conditions		
Opening Wall Temperature	300	K
Opening Wall	Pressure inlet	
Opening Wall Pressure	0	Pa
Opening wall do not participate in radiation		
Hot Wall Temperature	310	K
Hot Wall Material	Aluminum	
Hot wall emissivity	1	
Interior surface body material	Air	
ΔT	10	K
Insulation -Heat Flux boundary condition	0	W/m^2
Insulated wall emissivity	1	
Operating Conditions		
Operating Pressure	0	Pa
Gravity- Ra=E2	-0,13	m/s^2
Operating Temperature	300	K
Specified Operating Density	1,1771	kg/m^3

Solution Methods	
Pressure-Velocity Coupling	
Scheme	SIMPLE
Gradient	Least Square Cell Based
Pressure	Presto
Momentum	Second Order Upwind
Energy	Second Order Upwind
Solution Controls	
Default Values	
Residuals	
Continuity	10^{-3}
x-velocity	10^{-3}
y-velocity	10^{-3}
Energy	10^{-6}
Solution Initialization	
Standard Initialization	
Compute from	All zones

CURRICULUM VITAE

Name Surname : Selin Bilmez

Place and Date of Birth : Sivas / 21.05.1987

E-Mail : selin.bilmez@gmail.com

EDUCATION

- **B.Sc.** : 2010, Middle East Technical University, Science and Art Faculty, Chemistry
- **B.Sc.** : 2011, Middle East Technical University, Engineering Faculty, Aerospace Engineering
- **M.Sc.** : 2018, Istanbul Technical University, Graduate School of Science Engineering and Technology, Department of Aeronautics and Astronautics Engineering

PROFESSIONAL EXPERIENCE

- 2018- present Research and Development Engineering Specialist at GASSERO
- 2016-2018 Research and Development Engineering Specialist at MUTLU AKÜ
- 2014-2015 Project Engineer at Sistem Teknik Industrial Furnace A.Ş.
- 2012-2013 Design Engineer at Hexagon Studio A.Ş.